Volume 16
Number 22
14 June 2024
Pages 10487-10866

Nanoscale

rsc.li/nanoscale

ISSN 2040-3372

ROYAL SOCIETY OF CHEMISTRY

MINIREVIEW
Takamasa Tsukamoto
Recent advances in atomic cluster synthesis: a perspective from chemical elements

NCNST

Nanoscale

ROYAL SOCIETY OF CHEMISTRY

MINIREVIEW

View Article Online
View Journal | View Issue

Cite this: *Nanoscale*, 2024, **16**, 10533

Recent advances in atomic cluster synthesis: a perspective from chemical elements

Takamasa Tsukamoto [a,b,c]

Despite its potential significance, "cluster chemistry" remains a somewhat marginalized topic within the chemistry field. However, atomic clusters with their unusual and unique structures and properties represent a novel material group situated between molecules and nanoparticles or solid matter, judging from both scientific standpoints and historical backgrounds. Surveying an entire material group, including all substances that can be regarded as a cluster, is essential for establishing cluster chemistry as a more prominent chemistry field. This review aims to provide a comprehensive understanding by categorizing, summarizing, and reviewing clusters, focusing on their constituent elements in the periodic table. However, because numerous disparate synthetic processes have been individually developed to date, their straightforward and uniform classification is a challenging task. As such, comprehensively reviewing this field from a chemical composition viewpoint presents significant obstacles. It should be therefore noted that despite adopting a synthetic method-based classification in this review, the discussions presented herein could entail inaccuracies. Nevertheless, this unorthodox viewpoint unfolds a new scientific perspective which accentuates the common ground between different development processes by emphasizing the lack of a definitive border between their synthetic methods and material groups, thus opening new avenues for cementing cluster chemistry as an attractive chemistry field.

Received 21st December 2023,
Accepted 5th April 2024

DOI: 10.1039/d3nr06522g

rsc.li/nanoscale

1. Introduction

Atomic clusters comprising a few, a few dozen, or hundred atoms, with particle diameters of typically ~1 nm and reaching up to ~3 nm fall under an ultrasmall particulate material group (Fig. 1).

Compared to conventional nanoparticles (5–500 nm), their atypical smallness exhibits certain eccentric properties not found in nanoparticles, originating from the remarkable quantum size effect. Regarding general nanoparticles, physical properties and chemical reactivities are determined by their surface structures and geometrical shapes.[1–3] On the other hand, their electronic states of clusters resemble more closely those of molecules than bulk materials (including nanoparticles), leading to their unique characteristics.[4–8] Such clusters contribute to the manifestation of highly efficient and sophisticated biological functions in nature, such as water oxidation in photosynthesis, electron transfer, nitrogen fixation, and breathing.[9–13] Moreover, clusters possess various structural characteristics that are not observed in other chemicals, including the number of constituent atoms, types of constituent elements, elemental ratios, atomic arrangements, and geometrical symmetry. Such a feature affords a great degree of freedom in terms of material design. Furthermore, their steric and electronic structures on a molecular scale offer significant potential for achieving novel properties and functions. Therefore, this sub-nanometer material group has attracted worldwide attention as a candidate for next-generation post-nanotechnology materials.

However, the desired progress in the cluster chemistry field has been hindered by the inherent challenges entailed in synthesizing clusters, as compared to nanoparticles. This issue originates from the critical factors differentiating the pro-

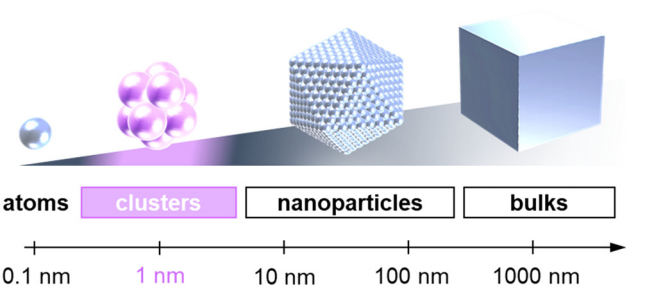

Fig. 1 Classification of materials based on the size scale.

[a]*Institute of Industrial Science, The University of Tokyo, 4-6-1 Komaba Meguro-Ku, Tokyo 153-8505, Japan. E-mail: ttsukamo@iis.u-tokyo.ac.jp*
[b]*Department of Applied Chemistry, School of Engineering, The University of Tokyo, 4-6-1 Komaba, Meguro-ku, Tokyo, 153-8505, Japan*
[c]*JST PRESTO, Honcho, Kawaguchi, Saitama, 332-0012, Japan*

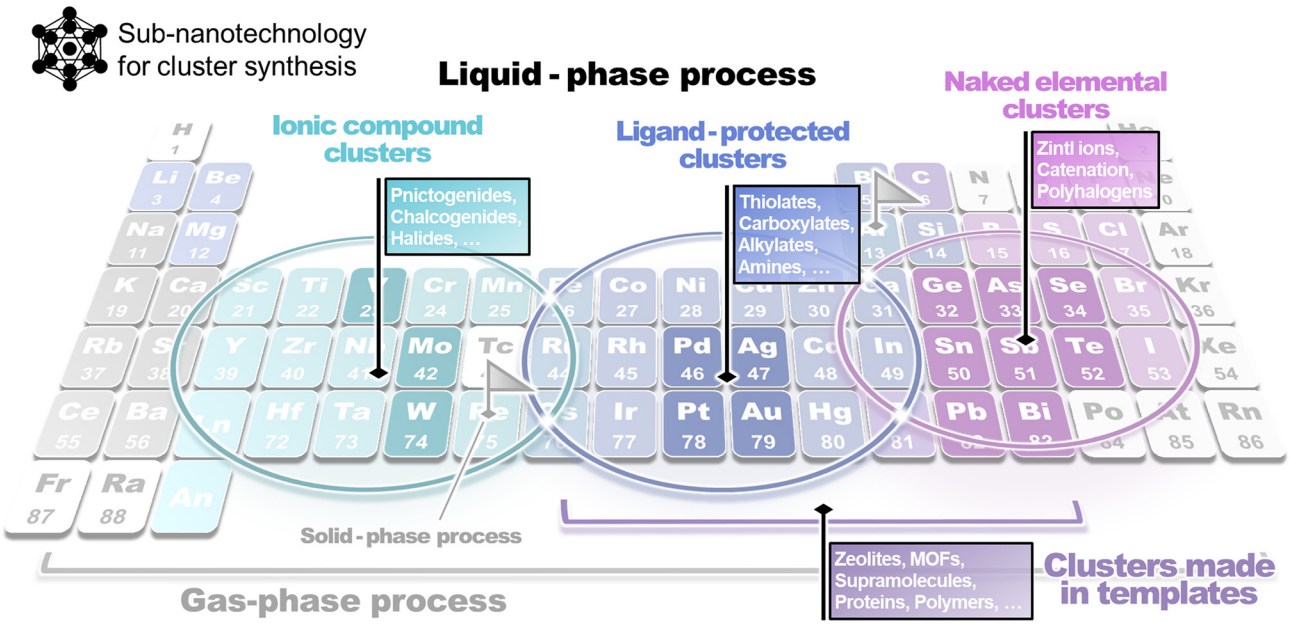

Fig. 2 A rough sketch of a map for the classification of suitable methods for atomic cluster synthesis depending on the chemical element composition.

perties of nanoparticles and clusters. Particularly, in contrast to nanoparticles, the structures, properties, and stabilities of clusters depend significantly on the number of constituent atoms. Since precise atom manipulation techniques (within 1 nm of the space in cluster particles) are necessary for the synthesis of clusters, applying conventional synthetic methods lacking atomic-level precision is unsuitable for forming such sub-nanosized materials. Therefore, developing new clustering techniques that are independent of these methods is essential. Atomic-level synthesis is significantly influenced by the nature of the constituent elements; however, in many cases, the types of elements that can be treated using a single method tend to be limited. By considering this aspect, synthetic methods dedicated to certain elements or elemental groups have been established, with the regions of the corresponding elements distributed on the periodic table like islands (Fig. 2). Notable developments in cluster chemistry have been achieved using these methods as starting points.

As noted above, synthetic methods for clusters, unlike those for nanoparticles, tend to be inflexible in terms of element selectivity and applicability, despite their high efficacy for a certain region in the periodic table. This limitation has hindered cross-cutting discussions focusing on constituent elements in the topic of cluster synthesis. In this review, with the aim of providing a comprehensive discussion and understanding of the entire field of cluster synthesis, we categorize, summarize, and review these methods by focusing on the constituent elements of clusters in the periodic table.

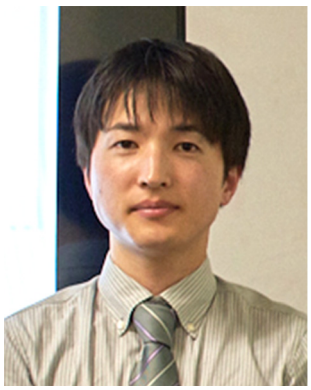

Takamasa Tsukamoto

Takamasa Tsukamoto received his PhD degree in Eng. from Tokyo Metropolitan University in 2015. After being a research fellow of the Japan Society for the Promotion of Science (2014–2016), a visiting researcher at the University of Miami (2014), a doctoral research fellow at the University of Tokyo (2015–2016), and a postdoctoral researcher and an assistant professor at the Tokyo Institute of Technology (2016–2023), he joined the Institute of Industrial Science at the University of Tokyo as a lecturer (2023) and the Japan Science and Technology Agency as a PRESTO researcher (2020–2023). His current research interests include developing organic–inorganic hybrid compounds for cluster synthesis, theoretical studies on clusters involving superatoms, the interpretation of the super-degeneracy phenomenon, and proposing a higher-order periodic table of superatoms.

2. Methods for cluster synthesis

Metal carbonyl clusters composed of single or multiple transition metal elements and carbonyl ligands represent one of the most well-established material groups among chemical clusters. They possess the most fundamental structures in coordination chemistry and serve as precursors in various chemistry fields, typified by organometallic chemistry.[14] These clusters are synthesized by common chemical reactions and

their reaction formulas are relatively simple. Moreover, borane clusters are also well synthesized mainly by the pyrolysis of diborane, and their atomicity and shape are classified as obeying the Wade–Mingos rule[15,16] or the Jemmis mno rule.[17]

However, in such cases, the degrees of freedom of design and synthesis are reduced and limited from the perspective of expanding the applicable elements. For example, in thermodynamically stable clusters obtained as metal carbonyls, the number of metal atoms, carbonyl ligands, and structures (hapticity) are uniquely determined by the electronic state of the transition metals. Therefore, the introduction of new factors that can be actively added or modified into the synthesis process of clusters is key for obtaining clusters composed of the desired number of atoms and element types. Based on this concept, various synthetic approaches using gas-, liquid-, and solid-phase reactions have been investigated.

3. Gas-phase synthesis

Fullerenes stand as the most well-known clusters synthesized in the gas-phase.[18–20] In an arc reactor or through laser vaporization in vacuum, fullerenes, typified by commercially available C_{60}, C_{70}, and C_{84} are obtained from carbon sources as a mixture and subsequently separated and purified by chromatography.

Endohedral fullerenes in which other elements are constrained in their cages, such as $[Li@C_{60}]^+$, can also be prepared using carbon mixed with metal sources.[21,22]

Although gas-phase synthesis is also effective in the case of heavier metal elements,[23] metal clusters tend to easily undergo aggregation and particle enlargement after production, in contrast to lighter elements. Therefore, techniques for separating clusters from mixtures directly after synthesis are crucial. In particular, gas-phase reaction systems combined with mass-separation units are often employed, leading to numerous reports on metal clusters typified by Na_x.[24] This method not only effectively yields single elemental clusters such as superatomic $[Al_{13}]^-$,[25] stannaspherene $[Sn_{12}]^{2-}$,[26] borospherene $[B_{40}]^-$,[27] and tetrahedral Au_{20},[28] but also heteroelemental clusters such as $M@Sn_{12}$[26] and $M@Si_{16}$.[29] On the other hand, stable extraction of clusters produced from the gas phase has recently been investigated, including the soft-landing method, in which clusters are deposited intact on a self-assembled monolayer (SAM) of alkyl groups formed on a substrate.[30]

As mentioned above, gas-phase preparation techniques offer the merit of involving the use of many elements, including both metal and nonmetal elements, but are fundamentally not conducive to mass production. Therefore, although these methods are significantly effective for analyzing physical properties, including electronic states, they are not suitable for investigations requiring large amounts of clusters, such as chemical reactivity. Additionally, because it is necessary to provide a positive or negative charge to clusters for mass separation, the properties of charged clusters are preferentially observed. The latter can be addressed by establishing a neutralization method for obtaining neutral clusters after mass separation.[31]

4. Liquid-phase synthesis

Various liquid-phase synthesis methods have been explored due to their practicality. The principal approaches for stabilizing clusters involve methods adopting ligand protection, employing polyoxometalate anions, and applying the Zintl phase. Each method targets specific regions of elements in the periodic table, leading to differences in the properties of the obtained clusters. These disparities often arise from variations in the chemical states of the clusters' surface or interior. Therefore, given the present circumstances, a suitable synthetic method should be carefully selected that not only considers the employed elements, but that can also induce the desired properties.

4.1. Clusters stabilized by ligand protection

In this method, the clusters are chemically stabilized by the steric and electronic protection effect of the organic ligands, which cover their surface atoms with functional groups. Applicable metal elements vary depending on the functional groups of the ligands. Negatively charged alkylthiolate-type (SR^-) ligands typically used for group 11 element clusters (Au, Ag, Cu) are among the most well-investigated representatives of this method.[32–36] Alkyl selenide-type analog structures (SeR^-) have also been reported.[37] The steric structure of ligands modifies the number of constituent atoms and their geometric arrangements, which are often based on highly symmetric core structures.[38] In this regard, $Au_{102}(SR)_{44}$,[39] $Au_{144}(SR)_{60}$,[40,41] $[Ag_{180}(SR)_{90}(CH_3SO_3)_{44}]^{46+}$,[42] and $Ag_{374}(SR)_{113}Br_2Cl_2$[43] stand as the largest well-known clusters with numerous constituent atoms (Fig. 3A). Recent reports have revealed that this method is also applicable to the synthesis of alloy clusters composed of group 11 elements, such as $[Au_{12}Ag_{32}(SR)_{30}]^{4-}$ (ref. 44) (Fig. 3B), despite the composition and arrangement of multiple elements in these clusters tending to be uncontrollable because of the preferential generation of energetically stable clusters. Additionally, an alloying method for doping with other metal elements has been developed by utilizing the stability of ligand-protected Au or Ag clusters.[45] This approach enables the use of metals that do not achieve ligand stabilization, such as $[M@Au_{25}(SR)_{18}]^-$ (M = Pd, Pt, Cd, Hg)[46] and $Pd@Ag_{20}(S_2PR_2)_{12}$[47] ($S_2P(OR)_2^-$ = dialkoxyldithiophosphinate). A recently reported anion-templated synthesis method of such clusters (especially for Ag clusters) also provides various geometric structures containing non-metallic elements or anionic species (atomic anion: H^-, D^-, F^-, Cl^-, Br^-, I^-, S^{2-}, Se^{2-}, and Te^{2-}; oxoanion: CO_3^{2-}, $C_2O_4^{2-}$, $C_4O_4^{2-}$, $C_5O_5^{2-}$, NO_3^-, AsO_4^{3-}, SO_3^{2-}, SO_4^{2-}, SeO_3^{2-}, SeO_4^{2-}, TeO_3^{2-}, TeO_6^{6-}, ClO_4^-, VO_4^{3-}, CrO_4^{2-}, MoO_4^{2-}, and WO_4^{2-}; polyoxometalate anion: $[V_{10}O_{28}]^{6-}$, $[Mo_6O_{22}]^{8-}$, $[EuW_{10}O_{36}]^{9-}$, *etc.*) in the center of the structure,[48] such as $[X@Ag_8(S_2P(OR)_2)_6]^{+/0}$ (X = F, Cl, Br, S).[49,50] Other elements in group 11 have also

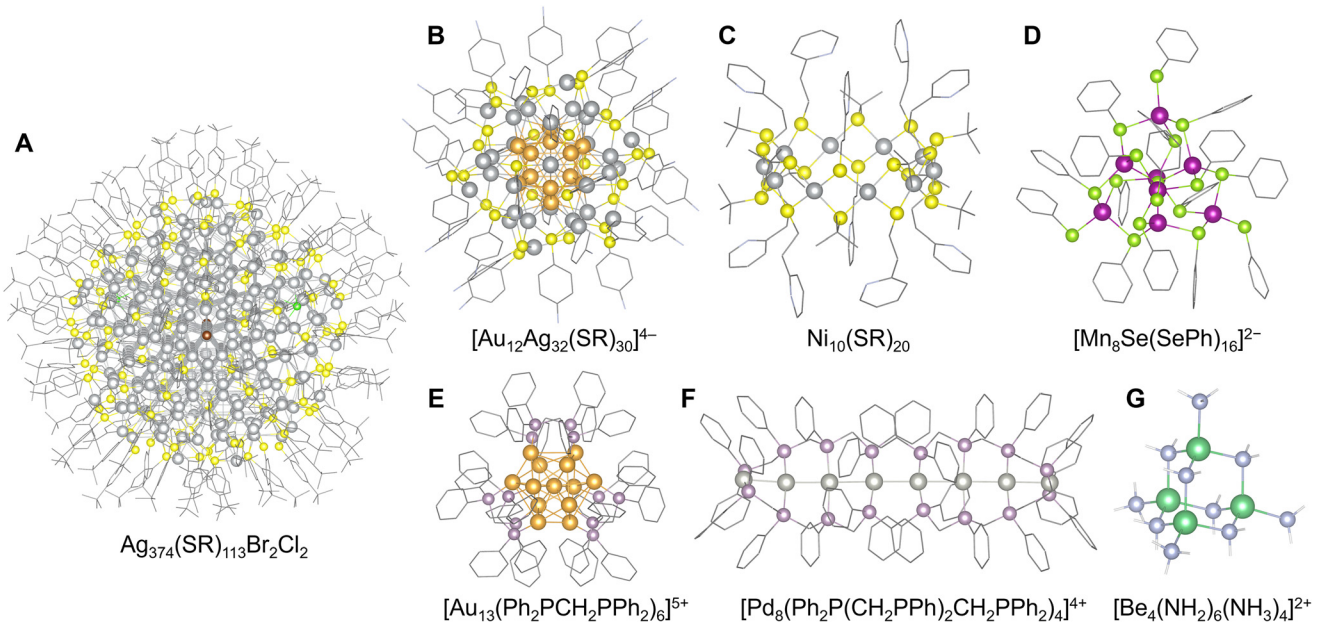

Fig. 3 Crystal structures of: (A) $Ag_{374}(SR)_{113}Br_2Cl_2$ (R = 4-tert-butylphenyl),[43] Ag: gray, S: yellow, Cl: green, Br: brown, and C: grayish bone; (B) $[Au_{12}Ag_{32}(SR)_{30}]^{4-}$ (R = 4-fluorophenyl),[44] Au: orange-yellow, Ag: gray, S: yellow, C: gray bone, and F: pale blue bone; (C) $Ni_{10}(SR)_{20}$ (R = 2-pyridylethyl),[52] Ni: gray, S: yellow, C: grayish bone, and N: pale blue bone; (D) $[Mn_8Se(SePh)_{16}]^{2-}$,[56] Mn: violet, Se: yellow-green, C: gray bone; (E) $[Au_{13}(Ph_2PCH_2PPh_2)_6]^{5+}$,[66] Au: orange-yellow, P: grayish pink, and C: grayish bone; (F) $[Pd_8(Ph_2P(CH_2PPh)_2CH_2PPh_2)_4]^{4+}$,[70] Pt: gray, P: grayish pink, C: grayish bone; and (G) $[Be_4(NH_2)_6(NH_3)_4]^{2+}$,[75] Be: green, N: pale blue, and H: white. Figures are reproduced from (A) CCDC 1496141, (B) CCDC 953881, (C) CCDC 743607, (D) CCDC 612696, (E) CCDC 1577669, (F) CCDC 1023572, and (G) CCDC 1982295.

been investigated, such as $[Cl@Cu_{14}(S(CH_3)_2(CH_2NH_2))_{12}]^{7+}$.[51] Thiolate-type ligands have also been used to stabilize metal sulfide clusters. For example, group 10 elements (Ni, Pd, Pt) form tiara-shaped cluster complexes, such as $[M(SR)_2]_n$ (M = Ni, Pd, Pt)[52–54] (Fig. 3C), that often encapsulate guest metal ions or molecules in their ring centers (I_2, Ag^+).[55,56] In the case of other group elements typified by Mn, Co, Zn, and Cd, a combination of monoanionic SR^- and dianionic S^{2-} provides sulfide clusters including tetrahedral $[Mn_8Se(SePh)_{16}]^{2-}$,[57] octahedral $[Co_8S_6(SPh)_8]^{4-}$,[58] tetrahedral $[Zn_{10}S_4(SPh)_{16}]^{4-}$,[59] and $[Cd_{54}S_{32}(SPh)_{48}(DMF)_4]^{4-}$ (ref. 60) (Fig. 3D).

Among other functional groups used for ligand protection, various neutral, cationic, and anionic ligands have been investigated. Neutral ligands typically include monodentate or multidentate organophosphines (PR_3), amines (NR_3), and imines (NR(=R)). Analogs with heavier atoms, such as organostibines (SbR_3), have recently been reported.[61] In the case of phosphines, clusters with group 11 elements, especially gold[62–65] (sometimes group 10 elements, such as $Ni_3(PPh)(PPh_2)_2(PPh_3)_3$[66]), typified by commercially available $[Au_3O(PPh_3)_3]^+$ and icosahedral $[Au_{13}(Ph_2PCH_2PPh_2)_6]^{5+}$ (ref. 67) are principally explored in the same manner as alkylthiolate (Fig. 3E). In particular, precisely designed multidentate phosphine ligands provide and control unique arrangements of metal atoms in a cluster, such as icosahedron-based $[Au_{20}(P(CH_2CH_2PPh_2)_3)]^{4+}$,[68] linear $[Au_4(Ph_2P(CH_2PPh)_2CH_2PPh_2)_2]^{4+}$ (ref. 69) and linear $[Pd_8(Ph_2P(CH_2PPh)_2CH_2PPh_2)_4]^{4+}$ with tetraphosphines[70] (Fig. 3F). Anion-templated synthesis is also used for clusters with phosphine ligands such as $Cl@Ag_{12}@Ag_{48}(Ph_2PCH_2PPh_2)_{12}$.[71] Another example is transition-metal chalcogenide clusters with protective ligands, such as $Co_6Te_8(PR_3)_6$.[72] The clusters were stabilized by amine or imine ligands: cubic $Cu_4I_4(C_5H_5N)_4$ with pyridine ligands,[73] rhombic $[In_4(C_{10}H_8N_2)_6]^{4+}$ with bipyridyl ligands,[74] and $[Be_4(NH_2)_6(NH_3)_4]^{2+}$ with ammonia ligands[75] (Fig. 3G).

Anionic ligands, including carboxylate ($OCOR^-$), represent a well-known example, especially for clusters with low atomicity. Examples include dinuclear clusters such as $M_2(OCOR)_4(L)_2$ (where M = Cr, Mo, Rh, Cu, Bi)[76] and trinuclear clusters such as $[M_3O(OCOR)_6(L)_3]^+$ (where M = V, Cr, Fe, Ru, Co, Rh, Ir).[77,78] Notably, such clusters are often commercially available. For the formation of these complex clusters, the oxidation number of the transition metal ions is an important factor; for example, dinuclear and trinuclear carboxylate clusters require metal ions with stable valences of +II and +III, respectively. In this regard, square-planar $V_4(OCOCH_3)_4(OH)_4(H_2O)_8$,[77] tetrahedral $Zn_4O(OCOCH_3)_6$, $Zn_{10}O_4(OCOCH_3)_{12}$[79] and $In_{37}P_{20}(OCOCH_2Ph)_{51}$[80] have been successfully reported. Alkoxides (OR^-), amides (NR_2^-), and methides (CR_3^-) have also been used as simple protecting ligands. In particular, research has primarily focused on group 13 and 14 elements (Al, Ga, In, and Sn).[81] Examples include $[Al_{77}(N(SiMe_3)_2)_{20}]^{2-}$ (ref. 82) and $Sn_{15}(NR_2)_6$,[83] while transition metal elements with structures resembling oxides are often crucial for alkoxides, as seen in compounds like $W_4(OR)_{16}$.[84]

Organometallic approaches are also effective in stabilizing clusters, with the formation of tetrahedral Li_4R_4 or octahedral Li_6R_6 clusters standing as a typical example.[85] In particular, cyclopentadienyl-type or pentamethylcyclopentadienyl-type ligands ($C_5H_5^-$ or $C_5Me_5^-$) have been extensively investigated for the stabilization of clusters composed of various elements. Typically, clusters of group 11, 12, and 13 elements (Cu, Zn, Al, Ga, and In) tend to have structures with large atomicity compared to transition metal elements (Co, Rh, Ir, *etc.*),[86] such as trigonal-bipyramidal $Zn_9(C_5Me_5)_6$[87] and tetrahedral $Al_4(C_5Me_5)_4$[88] (Fig. 4A). Alloy clusters have also been obtained using this method, such as trigonal-bipyramidal $Cu_3Zn_4(C_5Me_5)_5$,[89] with icosahedral $Cu_{43}Al_{12}(C_5Me_5)_{12}$ being one of the largest clusters reported to date[90] (Fig. 4B and C). Moreover, some transition metal halides, chalcogenides, and pnictogenides are also stabilized by cyclopentadienyl ligands like pseudo-tridecahedral $La_9I_{18}(C_5Me_5)_9$,[91] trigonal-bipyramidal $Rh_3Se_2(C_5EtMe_4)_9$,[92] and tetrahedral $Cr_4P_4(C_5Me_5)_4$[93] or $Mn_4P_4(C_5H_5)_4$[94] (Fig. 4D and E). Using this synthetic approach, model clusters mimicking the biochemical functions associated with nitrogen fixation were recently created (*e.g.*, $FeMo_3S_4(C_5H_4SiR_3)_3$).[95] Additionally, the aromatic rings with large π-conjugated systems also serve as a planar protection ligand and often provide sophisticated highly-symmetric clusters such as cuboctahedral $[Pd_{13}(C_7H_7)_6]^{2+}$ stabilized by cycloheptatrienylium ($C_7H_7^+$)[96] and square-planar $[Pd_4(C_8H_8)(C_9H_9)]^+$ stabilized by cyclooctatetraene (C_8H_8) and cyclononatetraenyl ($C_9H_9^-$)[97] (Fig. 5A). Conversely, bridged aromatic ligands can effectively stabilize group 11 elements (Au, Ag, and Cu), yielding star-shaped clusters typified by pentagonal planar $Au_5(C_6H_3Me_3)_5$, $Cu_5(C_6H_3Me_3)_5$, and square-planar $Ag_4(C_6H_3Me_3)_4$ with mesityl anions ($C_6H_2Me_3^-$)[98,99] (Fig. 5B). Additionally, tetramesityl diiron $Fe_2(C_6H_3Me_3)_4$ has also been reported, albeit not among group 11 elements.[100] Recently, by utilizing such bridged aromatic ligands, other atomic arrangements including alloys are obtained, like octahedral $[Au_4Ag_2(C_6H_4PR_2)_4]^{2+}$.[101] In contrast, aromatic ligands with bulky substituents also stabilize unique cluster structures by the steric protection effect, such as adamantane-shaped $Al_4(PH)_6(2,6\text{-}C_6H_4(C_6Me_3H_2)_2)_4$.[102]

Other organometallic approaches for controlling the number and arrangement of metal atoms in clusters have also been developed. For example, organosilicon or organogermanium ligands containing Si and Ge as metalloid elements yield group 10 metal clusters with unusual geometric structures, such as hexagonal planar $Pd_4(SiPh_2)_3((CH_2PH_2)_2)_3$ and hexagonal-bipyramidal $Pd_6(GePh_2)_2(CNC_6H_3Me_2)_{10}$[103–106] (Fig. 5C). Otherwise, the organometallic ligands form clusters, such as cyclic $(GeMes_2)_3$, $(GePh_2)_4$, and $(GePh_2)_5$ with Ge–Ge bonds[107–109] (Fig. 5D). Organic or organosilicon ligands have also been employed to synthesize clusters comprising nonmetallic C and semimetallic Si. For example, employing a low-

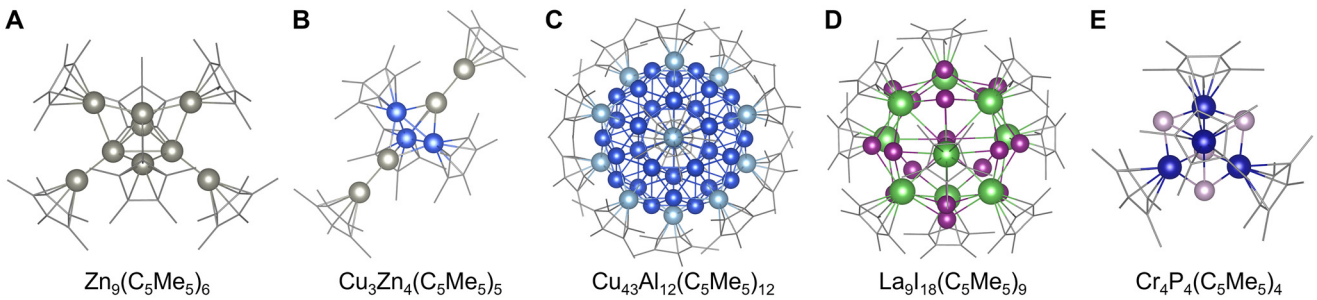

Fig. 4 Crystal structures of (A) $Zn_9(C_5Me_5)_6$.[87] (B) $Cu_3Zn_4(C_5Me_5)_5$,[89] (C) $Cu_{43}Al_{12}(C_5Me_5)_{12}$,[90] (D) $La_9I_{18}(C_5Me_5)_9$,[91] and (E) $Cr_4P_4(C_5Me_5)_4$.[93] Zn: gray, Cu: blue, Al: light blue, La: green, I: violet, Cr: dark blue, P: grayish pink, and C: grayish bone. Figures are reproduced from (A) CCDC 1434844, (B) CCDC 1854852, (C) CCDC 1845365, (D) CCDC 1992039, and (E) CCDC 984791.

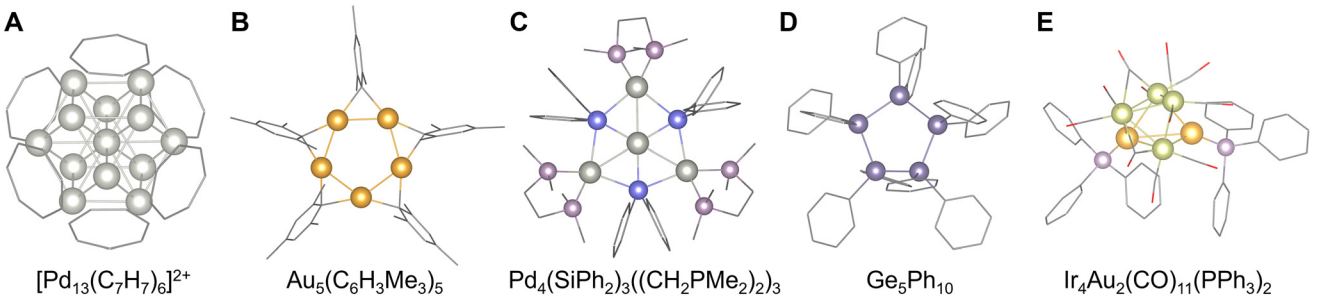

Fig. 5 Crystal structures of (A) $[Pd_{13}(C_7H_7)_6]^{2+}$,[96] (B) $Au_5(C_6H_3Me_3)_5$,[98] (C) $Pd_4(SiPh_2)_3((CH_2PMe_2)_2)_3$,[103] (D) Ge_5Ph_{10},[109] and (E) $Ir_4Au_2(CO)_{11}(PPh_3)_2$.[118] Pd: gray, Au: orange-yellow, Si: blue-violet, P: grayish pink, Ge: grayish blue-violet, Ir: light green-yellow, C: gray bone, and O: red bone. Figures are reproduced from (A) CCDC 1813458, (B) CCDC 1119882, (C) CCDC 702935, (D) CCDC 1137518, and (E) CCDC 924993.

temperature photochemical process or a pure organometallic process in a solvent can yield tetrahedral structures such as $C_4(CR_3)_4$ [110] and $Si_4(SiR_3)_4$.[111]

In other cases, methods for achieving both the stabilization and alloying of metal clusters using transition metal carbonyl complexes as ligands have been reported, such as octahedral $[Ag_{13}Fe_8(CO)_{32}]^{4-}$ (ref. 112) and three pentagonal-antiprismatic $[Sb_3Rh_{20}(CO)_{36}]^{3-}$ (ref. 113) complexes. It is worth mentioning that as a technique for clustering certain metals or mixing different metal elements in a cluster, the method using multiple ligands with different functional groups has been investigated, such as $Fe_8(N[o\text{-}H_2NC_6H_4NH(CH_2)_2]_3)_2(PMe_2Ph)_2$ with tetraamine and phosphine ligands,[114] $Ga_6(C_6Me_3H_2)_4(C_3N_2Me_2Pr_2)_2$ with mesityl and tetraalkylimidazol-2-ylidene ligands,[115] $[Mg_{16}(C_5Me_5)_8(NEt_3)_2Br_4]^{2-}$ with cyclopentadienyl and amine ligands,[116] $Cu_{10}Zn_2(C_6Me_3H_2)_6(C_5Me_5)_2$ with mesityl and cyclopentadienyl ligands,[117] $Ir_4Au_2(CO)_{11}(PPh_3)_2$,[118] $Pt_{13}Au_4(CO)_{10}(PPh_3)_8$,[119] and $Pd_{145}(CO)_x(PEt_3)_{30}$ ($x \approx 60$)[120] with carbonyl and phosphine ligands (Fig. 5E), and co-crystalized $[(AuAg)_{267}(SPhMe_2)_{80}]\cdot[(AuAg)_{45}(SPhMe_2)_{27}(PPh_3)_6]$ with thiolate and phosphine ligands.[121] This approach has recently led to the development of model clusters for photosynthetic systems (Mn_3Ca clusters with carboxylate and pyridine ligands).[122]

By surveying ligand protection methods, we can broadly summarize the tendencies of the applicable elements for each method. The most extensively studied elements in ligand protection methods are noble metals (Pd, Pt, Au, and Ag). Following closely are other late transition metal elements (Fe, Co, Rh, Ni, Cu) and post-transition elements (Zn, Cd, Al, Ga, and In). Remarkably, the bond type between the metal atoms directly influences the diversity of the cluster structures. The fact that the most varied cluster structures were found for the metal elements in group 11 could be rationalized by their valence *s*-electrons forming relatively free bonds and resistance to oxidation. In contrast, other elements tend to be in charged states with the ligands. Although there are relatively few reports on minor elements, a few atoms are often implemented in a cluster by doping the surrounding environment where the stabilization effect of cluster structures composed of major elements is dominant. The types of elements stabilized as a cluster significantly differ by and depend on the functional groups of the organic ligands, which are frequently observed in the case of clusters with single-bond-mediated ligand protection. However, only cyclopentadienyl ligands differ from these ligands and are utilized for applying a broad range of elements by stabilizing clusters with both electrostatic and steric effects. Therefore, such an approach, without obvious single-bond-mediated ligand protection, is expected to be effective for developing versatile synthetic methods from the viewpoint of applicable elements.

Although simple functional groups such as thiolates, carboxylates, and phosphines are used in conventional methods, suitable ligands for this approach are being explored and developed. In particular, new ligands with more complicated structures and compositions containing multidentate ligands afford unique stability to cluster structures.[123] Such a method to stabilize a certain geometric structure using custom-designed multidentate ligands is similar to the approach for controlling crystal polymorphs of nanoparticles, in which modification of the surface of a nanoparticle by multidentate ligands induces unusual crystal structures in the whole nanoparticle.[124] These reports also indicated that an approach that induces multipoint interactions between a cluster and its ligands is effective for developing versatile synthetic methods.

4.2. Clusters stabilized as ionic compounds

Clusters solely stabilized without protecting ligands have also been reported. They are generally obtained as ionic compounds that undergo electronic stabilization by bonding with pnictogens, chalcogens, halides, and metals with lower electronegativity. Polyoxometalate (POM) clusters are well-known materials. These clusters are almost negatively charged metal oxides and tend to be composed of metal atoms with high oxidation numbers.[125–127] In many cases, group 5 and 6 elements (V, Nb, Ta, Mo, and W) in the +V or +VI state prefer a six-coordination state. Some species such as paramolybdate $[Mo_7O_{24}]^{6-}$, decatungstate $[W_{10}O_{32}]^{4-}$, metatungstate $[W_{12}O_{40}]^{8-}$, paratungstate $[W_{12}O_{42}]^{12-}$, molybdenum blue reagents $[Mo_{154}O_{462}H_{14}(H_2O)_{70}]^{14-}$ and $[Mo_{152}O_{457}H_{14}(H_2O)_{68}]^{16-}$ are commercially available.[128] $[H_xMo_{368}O_{1032}(H_2O)_{240}(SO_4)_{48}]^{48-}$ was one of the largest POM clusters[129] (Fig. 6A). Similarly, group 3 superheavy elements (U, Np, Pu, and partially Am) in the +V or +VI state also form POM structures, such as $[U_{60}O_{240}(OH)_{60}]^{60-}$ with fullerene topologies[130–132] (Fig. 6B). The atomicity and arrangement of POM clusters can often be tuned by introducing other elements as the central core. For example, 4-coordinating species mainly in group 13, 14, and 15 elements (B, Al, Ga, C, Si, Ge, P, and As), such as PO_4^{-}, SiO_4^{2-}, and AlO_4^{3-} species, form unique structures typified by tungstophosphate $[PMo_{12}O_{40}]^{3-}$ called Keggin-type structures.[125,126] Fe, Co, Cu, and Zn in the +II or +III state, and S and Se in the +VI state have also been reported as tetrahedral centers. In the case of 6-coordinating species of elements (Cr, Mn, Fe, Co, Rh, Ir, Ni, Pd, Pt, Cu, Zn, Al, Ga, Sb, Te, I), more planar Anderson–Evans-type POM clusters are constructed by a central EO_6 unit that is often in highly oxidized states, such as $[CoMo_6O_{18}(OH)_6]^{6-}$ with Co(+III), $[PtW_6O_{24}]^{8-}$ with Pt(+IV), and $[IMo_6O_{24}]^{8-}$ with I(+VII).[124,133] Moreover, icosahedrally 12-coordinating EO_{12} central units containing group 3 and 4 heavy elements (Ce, Th, U, Np, and Zr in the +IV or +V state) provide unique Dexter–Silverton-type structures such as pyritohedral $[CeMo_{12}O_{42}]^{8-}$.[134] By introducing two or more core units, POMs lead to the construction of more complicated structures called Wells–Dawson-type or Preyssler–Pope–Jeannin-type structures.[125] Additionally, multiple POMs form sandwich-type or capsule-type structures intercalating group 1, 2, and 3 elements and low valent transition metals as a cation,[125,135] and they are also found in natural minerals, typified by the $[Zn_2Mn_2(H_2O)_2(FeW_9O_{34})_2]^{12-}$ cluster in ophirite.[136] By applying this unique property that partially incorporates other elements in or between POMs, it is possible to synthesize

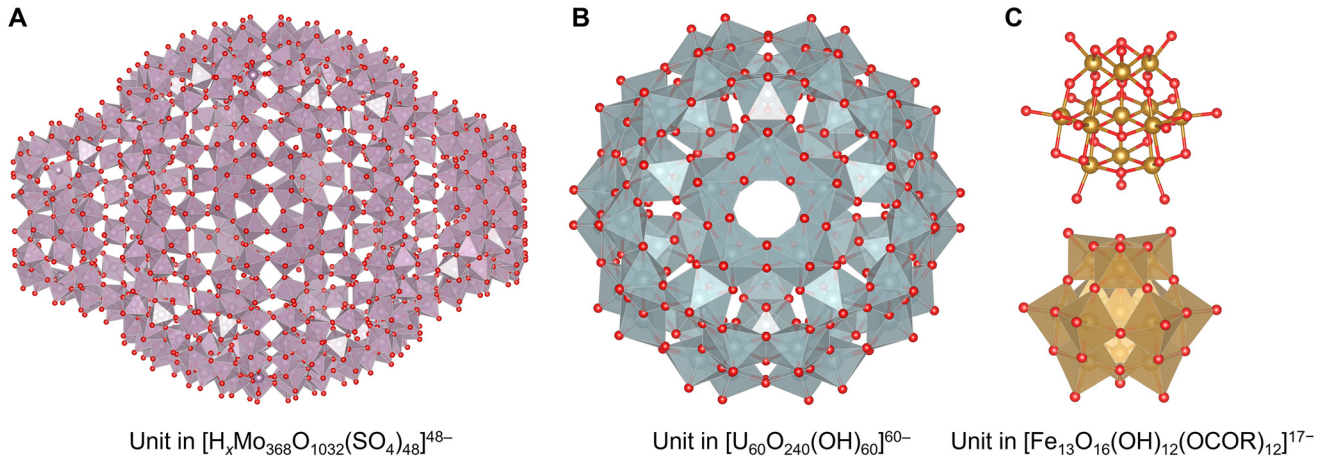

Fig. 6 Crystal structures of (A) a unit in $[H_xMo_{368}O_{1032}(H_2O)_{240}(SO_4)_{48}]^{48-}$ with a structure showing molybdenum oxide polyhedra,[129] (B) a unit in $[U_{60}O_{240}(OH)_{60}]^{60-}$ with a structure showing uranium oxide polyhedra,[130] and (C) a unit in $[Fe_{13}O_{16}(OH)_{12}(OCOR)_{12}]^{17-}$ with a structure showing iron oxide polyhedra (below).[142] Mo: reddish gray polyhedron, O: red, U: bluish gray polyhedron, Fe: brown, and O: red. Figures are reproduced from (A) CCDC 1727624, (B) CCDC 1732644, and (C) CCDC 1525080.

rarer, larger and more complicated structures, such as tetrapod-shaped $[Ti_4Cl(OH)_{12}(P_2W_{15}Ti_3O_{62})_4]^{45-}$ where Ti atoms are sandwiched by four POM cluster units,[137] wheel-shaped $[Cu_{20}Cl(OH)_{24}(H_2O)_{12}(P_8W_{48}O_{184})]^{25-}$ where Cu atoms are encapsulated in a circular POM cluster host,[138] and a tetrahedral layered superstructure of $[La_{10}Ni_{48}W_{140}Sb_{16}P_{12}O_{568}(OH)_{24}(H_2O)_{20}]^{86-}$.[139] Recently, it was reported that large capsule-like POM clusters can also incorporate other small metal clusters into their centers, such as $[Ag_{27}@(Si_2W_{18}O_{66})_3]^{31-}$.[140]

With the exception of V, Mo, and W, advanced synthesis techniques have been developed. In particular, the polycationic Keggin-type structures of aluminum $[Al_{30}O_8(OH)_{56}(H_2O)_{24}]^{18+}$ containing 6-coordinating AlO_6 sites and central 4-coordinating AlO_4 sites are well known.[141] However, in such cases, co-adoption of the concept of ligand protection in these clusters is also effective in synthesizing POMs composed of minor elements, such as Keggin-type $[Fe_{13}O_{16}(OH)_{12}(OCOR)_{12}]^{17-}$ containing an Fe(+II) center and Fe(+III) shells with carboxylate ligands[142] (Fig. 6C), Keggin-type $[Mn_{13}O_6(OH)_2(OMe)_4L_6]^{4+}$ containing a Mn(+III) center and Mn(+IV) shells with alkoxylate and imine ligands (L = 2,6-bis[*N*-(2-hydroxyethyl)iminomethyl]-4-methylphenol),[143] $Ti_{17}O_{24}(OiPr)_{20}$ with alkoxylate ligands,[144] and octahedral $[(BuSn)_{12}O_{14}(OH)_6]^{2+}$ with alkyl ligands.[145] In contrast, a few POMs composed of only four-coordinating units are reported including $[Mn_{39}O_{55}]^{26-}$ (ref. 146) (Fig. 7A). Interestingly, the anion-templated synthesis described in the section on ligand-protected noble metal clusters is also effective for the synthesis of POM clusters. The geometries and charges of the template anion provide clusters with various sophisticated core–shell structures, such as $[(SCN)@HV_{22}O_{54}]^{6-}$, $[(CH_3COO)@H_2V_{22}O_{54}]^{7-}$,[147] $[Cl@Eu_{15}(OH)_{20}]^{24+}$,[148] and $[(SO_4)@As_4Mo_6V_7O_{39}]^{4-}$.[149] Even electronically neutral chemical species, such as solvent molecules, often serve as templates. For example, water and acetonitrile molecules compose $[(H_2O)@V_{18}O_{42}]^{12-}$ (ref. 150) and $[(CH_3CN)@V_{12}O_{32}]^{4-}$,[151] respectively.

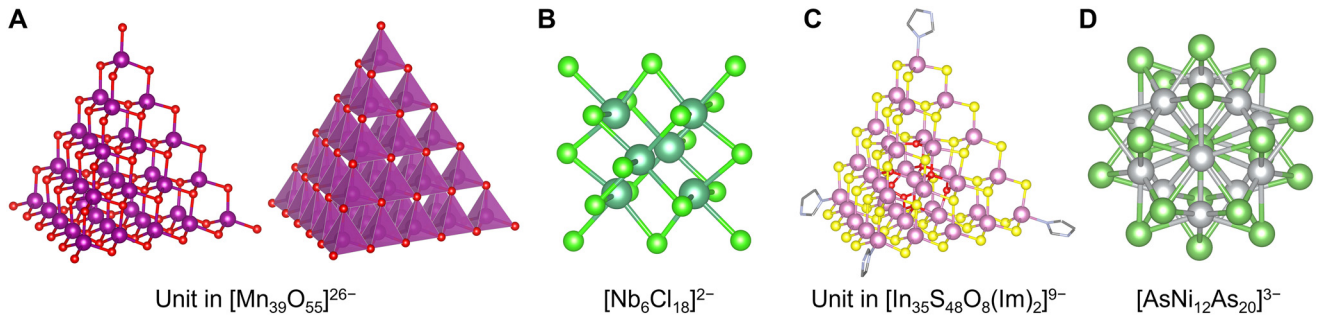

Fig. 7 Crystal structures of (A) a unit in $[Mn_{39}O_{55}]^{26-}$ with a structure showing manganese oxide polyhedra (right),[146] (B) $[Nb_6Cl_{18}]^{2-}$,[152] (C) a unit in $[In_{35}S_{48}O_8(Im)_2]^{9-}$,[153] and (D) $[AsNi_{12}As_{20}]^{3-}$.[155] Mn: reddish violet, O: red, Nb: bluish green, Cl: light green, In: pale magenta, S: yellow, Ni: gray, As: green, C: grayish bone, and N: light blue bone. Figures are reproduced from (A) CCDC 1728352, (B) CCDC 654117, (C) CCDC 1862551, and (D) CCDC 206301.

Except for the stabilization of clusters, such as the oxides mentioned above, other pnictogenides, chalcogenides, and halides can induce such stabilization. Polyhalometalate clusters, especially of early transition metals (Zr, Hf, Nb, Ta, Mo, W, Re), are well-known, such as $[Nb_6Cl_{18}]^{2-}$ (ref. 152) (Fig. 7B). The compound clusters also often have larger layered structures, such as tetrahedral $[In_{35}S_{48}O_8(Im)_2]^{9-}$,[153] tetrahedral $[Sn_{10}O_4S_{20}]^{8-}$,[154] icosahedral $[AsNi_{12}As_{20}]^{3-}$,[155] and tetrahedral $Sc_4C_{10}Sc_{20}I_{30}$ [156] (Fig. 7C and D). Additionally, it has been reported that the cation-templated synthesis of some chalcogenide clusters provides rare geometric structures, such as $[(NH_4)@Pd_2S_{28}]^{4-}$ (ref. 157) and $[Na_2@Fe_{18}S_{30}]^{8-}$.[158]

In summary, in the case of clusters obtained as ionic compounds, the oxide clusters of the early transition metals (V, Mo, and W) are the most investigated, and the runner-up is another base metal element with a relatively high valence (Al, Ti, Mn, Fe, and U). Halide clusters of early transition metals (Zr, Nb, Mo, Hf, Ta, W, and Re) are the main compounds used in this field. Similar to ligand-protected clusters, the introduction of minor elements is achieved by doping a few atoms into the cluster structure composed of major elements. Particularly for POM clusters, it appears that metal elements in remarkably high oxidation states play an important role in diversifying their steric structures. One factor is that metals with high oxidation states maintain the charge balance of the entire cluster structure by reducing the negative charge on their own metalate units. If the metalate anion is represented as $\{M^nO_6\}^{(12-n)-}$, its total negative charge is smaller when oxidation state n is higher. On the other hand, because the stability of these clusters is significantly associated with the affinity of the metal elements for pnictogens, chalcogens, and halogens, clusters composed of noble metals have rarely been reported. As represented by POMs, these clusters often have unique symmetric structures, whereas in the case of different metal elements, these metal oxide units tend to undergo atomic-level phase separation in a cluster and do not form true complex oxides with a uniform atomic co-arrangement. This suggests that the variety of ionic compound clusters can be expanded by improving the synthetic schemes.

4.3. Naked elementary clusters

In contrast, naked clusters composed only of icosagens, tetrels, pnictogens, chalcogens, and halogens (groups 13, 14, 15, 16, and 17) are also well known. Although white phosphorus (tetrahedral P_4) is the most famous example, it is generally an ionic species called Zintl clusters or Zintl ions that is stabilized in crystals.[159] In particular, there are many reports of Zintl clusters of group 13, 14, 15, and 16 metal elements with various polyhedral structures, such as icosahedral $[Tl_{13}]^{10-}$,[160] trigonal-bypyramidal $[Sn_5]^{2-}$,[161] bicapped-square-antiprismatic $[Pb_{10}]^{2-}$,[162] square antiprismatic $[Bi_8]^{2+}$,[163] square-planar $[Te_4]^{2+}$, and barrel-shaped $[Te_8]^{2+}$ (ref. 164) (Fig. 8A–C). In other cases, examples of clusters made of group 11, 12, and 17 elements are slightly known like icosahedral $[Ag_{13}]^{4+}$ (ref. 165) or polyhalogen cations and anions typified by rectangular $[Cl_4]^+$ (ref. 166) and trigonal-pyramidal $[I_7]^-$ (ref. 167) (Fig. 8D and E). Similar to other methods, Zintl clusters also form molecular alloys (intermetalloids) of such elements including $[BiIn_8Bi_{12}]^{3-/5-}$ (ref. 168) and $[K_2Zn_{20}Bi_{16}]^{6-}$,[169] or clusters incorporating a few other transition metal elements[170] including $[Sn_9Pt_2(PPh_3)]^{2-}$, $[Sn_9Ni_2(CO)]^{3-}$ (ref. 171) and $[Th@Bi_{12}]^{4-}$ (ref. 172) with and without protecting ligands, respectively (Fig. 8F and G).

As mentioned above, these clusters are mainly composed of post-transition elements with many valence electrons, and in many cases, they are positively or negatively charged structures. This tendency is rationalized by the thermodynamic stability based on the electronic configurations unique to clusters typified by superatoms.[6–8,25,32,36,47,90] These clusters generally have relatively rigid structures with large bond angles of up to 90° originating from *p*-electrons and the ability to contain a few atoms of other group elements in electronically stabilized skeletons. In particular, the endohedral structures typified by stannaspherenes mentioned in the gas-phase synthesis section enable the incorporation of other groups of elements without ligands. It should be noted that the accurate choice of counter ions is an important factor in the stable design of these clusters because most clusters are obtained only in the crystal form.

4.4. Clusters obtained by nanospace-assisted template synthesis

The third method utilizes nanospace as reaction fields for cluster synthesis. Because the aforementioned synthetic methods depend on the thermodynamic stability of the cluster structure, only certain clusters with energetically suitable

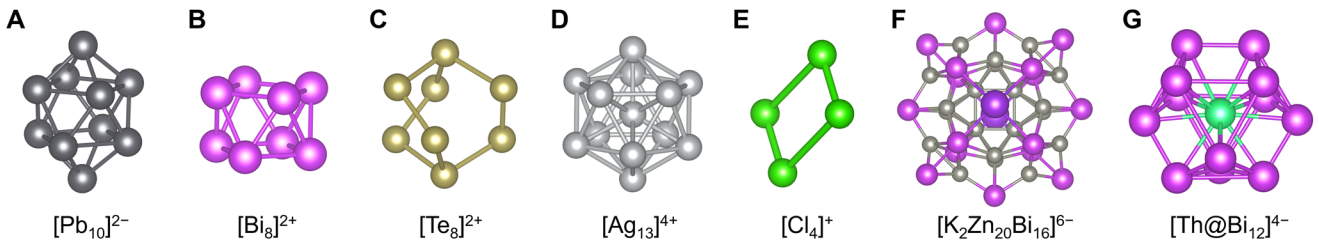

Fig. 8 Crystal structures of (A) $[Pb_{10}]^{2-}$,[162] (B) $[Bi_8]^{2+}$,[163] (C) $[Te_8]^{2+}$,[164] (D) $[Ag_{13}]^{4+}$,[165] (E) $[Cl_4]^+$,[166] (F) $[K_2Zn_{20}Bi_{16}]^{6-}$,[169] and (G) $[Th@Bi_{12}]^{4-}$.[172] Pb: black, Bi: purple, Te: grayish yellow, Ag: pale gray, Cl: light green, K: violet, Zn: gray, and Th: bluish green. Figures are reproduced from (A) CCDC 288640, (B) CCDC 1728864, (C) CCDC 1471867, (D) CCDC 1728248, (E) CCDC 1726993, (F) CCDC 1969162, and (G) CCDC 1983072.

atomicity, atomic arrangement, and composition ratios were obtained. However, in this method, the reaction field is confined within a nanosized space using various approaches, and unique clusters in metastable states that are not found using other methods are forcibly obtained. The pores of zeolites serve as typical capsules for cluster synthesis, such as tetrahedral $[Ag_4(H_2O)_4]^{2+}$ in their cages.[173–177] Metal–organic frameworks (MOFs) are also used for nanosized cages, and templated synthesis of various clusters, including Pt quasi-linear $[Pd_4]^{2+}$,[178] tetrahedral Ir_4,[179] $Pt_{12\pm x}$,[180] and triple-decker trigonal $[Au_3L_3\text{-}Ag\text{-}Au_3L_3\text{-}Ag\text{-}Au_3L_3]^{2+}$,[181] has been reported. Recently, MOFs have been used to cluster carbon as a nonmetal element through selective template synthesis of polyacenes using reactants.[182] Flexible supramolecular capsules realize the synthesis of such metastable clusters, including some allotropes of nonmetal elements, such as phosphorus P_4 [183] and sulfur S_6 or S_{12},[184] where the catenation behavior is controlled. In other cases, cages of crystalline proteins and nanospaces of macromolecules have been used as templates and protectors for clusters.[185,186] In such cases, because the precision of cluster synthesis depends on the operation of the atomic assembly, it is expected that only one method will allow us to use a broad range of elements by adopting the same chemical principle for the assembly. Indeed, the atom hybridization method utilizing multimetallic multinuclear complexes of dendrimers as macromolecular templates for cluster synthesis affords the highest degrees of freedom in the design of multielemental clusters.[187–191] Because it adopts the coordination behavior of guests for metal assembly based on the simple principle of acid–base chemistry, all elements can be treated under the same conditions during cluster synthesis. This approach led to the first synthesis of multimetallic clusters containing five or six metal elements like $GaInAu_3Bi_2Sn_6$.[187]

In contrast to other liquid-phase synthesis methods, template synthesis provides clusters with relatively metastable structures, which are also regarded as intermediates in the process producing more stable clusters. Capsules need to be individually designed for each chemical element, while this approach, which reduces the direct influence originating from the properties of the elements, enables the use of a broad range of elements. Alternatively, in this method, the interaction between the capsules and precursor compounds, such as electrostatic interactions, acid–base reactions (including coordination), and hydrophobic interactions, is a key factor for accumulating atoms. However, it is important to stabilize such clusters in order to hold them in capsules or fix them on/in support materials. Moreover, in many cases, it is difficult to conduct the usual identification analyses, such as single-crystal X-ray diffraction and direct observation by STEM, SPM, and MS, which are often effective.

5. Solid-phase synthesis

Several methods have been reported for the synthesis of clusters in the solid phase. The mechanochemical synthesis of general nanoparticles has already been established, but that of clusters remains limited.[192] For instance, Keggin-type POM of aluminum $[Al_{13}O_4(OH)_{24}(H_2O)_{12}]^{7+}$ can be obtained by a mechanochemical reaction between the $[Al(H_2O)_6]Cl_3$ and $(NH_4)_2CO_3$ reactants.[193] Dimensional reduction of solid-state precursors is effective for the precise synthesis of clusters. Some metal chalcogenide or halide clusters typified by $[Re_6S_6Cl_8]^{2-}$ are stoichiometrically synthesized by dimensional reduction of an extended solid-state structure.[194,195] As an ultimate physical method, a technique for the mechanical synthesis of clusters by directly manipulating atoms using scanning probe microscopy was recently developed. Indeed, metal clusters such as Au_{12}, Ag_{12}, and Au_5Pb have been synthesized directly on Si surfaces.[196]

As mentioned previously, the advantages of synthetic methods involving solid-phase processes are extremely limited in terms of the selectability of elements. However, bottom–up synthesis involving mechanochemical reactions and top–down synthesis involving dimensional reduction are significantly more effective for mass production than liquid-phase synthesis. This suggests that expanding the applicable elements in solid-phase synthesis will contribute to promoting clusters as more general and valuable materials in the future.

6. Conclusions and perspectives

As discussed above, the optimal method for synthesizing clusters varies significantly depending on the chemical element involved. Consequently, research on cluster synthesis has been pursued individually, with each method serving as a starting point. Notably, in liquid-phase processes, doping other group elements using the stable structures and atomic-level space obtained by each method has proven highly effective. Recently, these methods have been increasingly interconnected based on this approach.

However, according to the classification of clusters based on chemical elements, it is evident that there is no accurate border between cluster structures, even though each adopts a different synthetic method. For example, certain representatives among ligand-protected clusters and ionic compound clusters, namely $[Be_4(NH_2)_6(NH_3)_4]^{2+}$,[75] $[Zn_{10}S_4(SR)_{16}]^{4-}$,[59] $Zn_{10}O_4(OCOR)_{12}$,[79] $In_{37}P_{20}(OCOCH_2Ph)_{51}$,[80] $[Mn_{13}O_6(OH)_2(OMe)_4L_6]^{4+}$,[143] and $[In_{35}S_{48}O_8(Im)_2]^{9-}$,[153] partially contain both their two structural factors for cluster stabilization. $[Sn_9Pt_2(PPh_3)]^{2-}$ (ref. 171) can be regarded as a cluster undergoing stabilizing effects by both ligand-protection and Zintl anions. Interestingly, the clusters developed using different methods often exhibit similar structures with reversed atomic arrangements and elemental ratios. Some of the simplest examples are $[Co_8S_6(SPh)_8]^{4-}$ (ref. 58) and $Co_6Te_8(PR_3)_6$,[72] where the transition metal and chalcogen atoms occupy reversed positions in the same symmetric structure. Moreover, $[Sb_3Rh_{20}(CO)_{36}]^{3-}$ reported as a ligand-protected cluster with a few free post-transition metal atoms[113] and $[Sn_9Ni_2(CO)]^{3-}$ reported as a Zintl cluster with a few

ligand-protected transition metal atoms[171] have a complementary relationship (Fig. 9A). Additionally, the $[Mo_6O_{22}@Ag_{58}S_2(SPhtBu)_{36}(OCOCF_3)_{10}]$ cluster obtained by the anion-template synthesis of ligand-protected clusters[48,197] and the $[Ag_{27}@(Si_2W_{18}O_{66})_3]^{31-}$ clusters obtained by the expansion of the synthesis method of POMs[140] also have complementary structures. In their skeletons, where the $[Mo_6O_{22}]^{8-}$ POM unit was encapsulated in a ligand-protected Ag_{58} cluster and the $[Ag_{27}]^{17+}$ unit was encapsulated in three open-Dawson-type POMs $[Si_2W_{18}O_{66}]^{16-}$, the core and shell structures were completely inverted (Fig. 9B). $Ag_6@(MoO_4)_7@Ag_{56}(MoO_4)_2(SiPr)_{28}(p\text{-}SO_3PhMe)_{14}$ with a nested structure was recently synthesized.[198] This similarity and reversibility of the cluster structures indicate that the area of elements covered by each synthetic method has been extended widely enough to be close to each other in recent investigations. This suggests that a more flexible cluster design can be realized in the future by improving synthetic techniques.

However, there are uninvestigated clusters for which precise synthetic methods that allow mass production, such as multimetallic clusters, have not yet been established. In light of the tendencies mentioned above, blending these individually developed synthetic methods is expected to make a breakthrough in revealing as-yet-unknown clusters. Although such an attempt has already been made, for example, the combination of ligand protection and nanospace-assisted synthesis methods,[199] reports are still rare.

The electronic analogy between the clusters obtained using different methods suggests the possibility of new cluster structures by isomorphic substitution. For example, the ligand-protected $[M(SR)_2]_n$ (M(II) = Ni, Pd, Pt) in section 4.1 might provide as-yet-unknown tiara-type bimetallic clusters, such as $[M(SR)_2]_n[M'S_2]_x$ (M(III) = Mn, Fe, In), by doping based on the concept of chalcogenide clusters. Borane and Zintl clusters often have very similar geometric structures according to the Wade–Mingos rule,[15,16] such as square pyramidal B_5H_9 [200] and $[In_5]^{9-}$ (ref. 201) or bicapped-square-antiprismatic $[B_{10}H_{10}]^{2-}$ (ref. 202) and $[Pb_{10}]^{2-}$.[162] As some transition-metal elements doped with ligands have been reported,[171,203] mutual feedback from each chemistry associated with the synthetic methods will become an effective approach for designing new cluster structures. Cation- or anion-templated methods will also contribute to the creation of such hybridized clusters because they are reported in both ligand-protected clusters and ionic compound clusters. Although conventional clusters obtained by ion-templated synthesis are composed of relatively simple anions as core structures, undeveloped ionic species of metals or metal oxides allow expandability in their structures. For example, by tracing these methods, the templated synthesis of clusters adopting uninvestigated ions, such as Ni^{2+}, Zn^{2+}, VO^{2+}, RuO_4^-, and $[Pt(OH)_6]^{2-}$, may contribute to creating clusters with new combinations of elements. Additionally, the secondary chemical treatment of these clusters, inspired by nanospace-assisted synthesis, is expected to add new lineups, even in Zintl clusters. Unrevealed pure metal clusters typified by such Zintl clusters will be obtained by the reduction of ionic compound clusters with diverse structures typified by POMs as precursors.

In contrast to clusters, synthesis methods for nanoparticles cover a broad range of chemical elements and chemical fields.[1] Therefore, hybridizing conventional synthesis methods for nanoparticles and clusters is expected to contribute significantly and provide new guidelines for cluster synthesis. As described in the sections on ligand-protected clusters, modifying the cluster structures with multidentate ligands is a strong candidate.[123,124] The effectiveness of such an approach following the methods for nanoparticles might ultimately be extended to bulk materials containing clusters as partial structures, such as clathrate compounds, gas hydrates, or minerals[204–208] and cluster units in metallic glasses or quasi-crystals.[209–213]

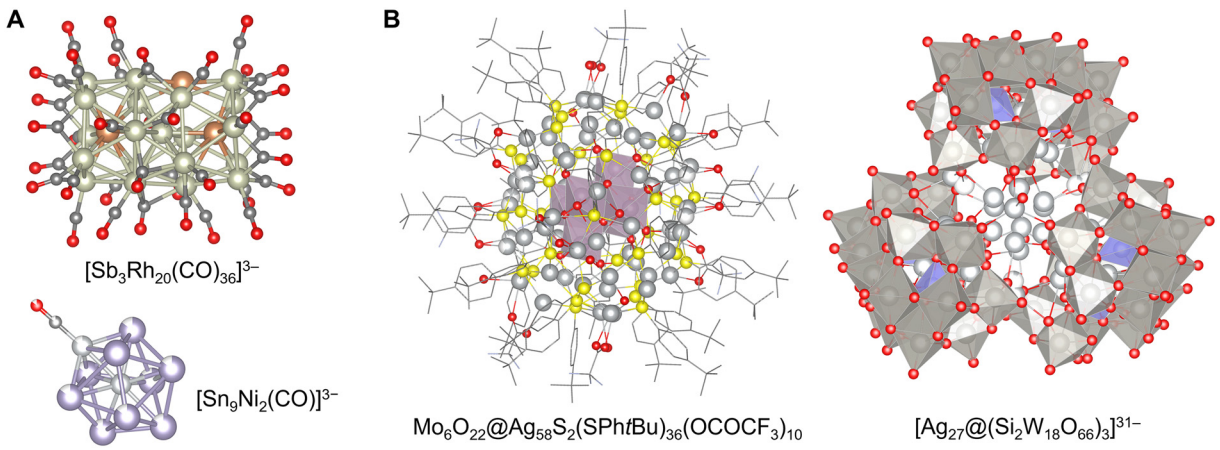

Fig. 9 (A) Crystal structures of $[Sb_3Rh_{20}(CO)_{36}]^{3-}$ (ref. 113) and $[Sn_9Ni_2(CO)]^{3-}$,[171] C: gray, O: red, Ni: light gray, Rh: grayish green, Sn: pale purple, and Sb: brown. (B) Crystal structures of $Mo_6O_{22}@Ag_{58}S_2(SPhtBu)_{36}(OCOCF_3)_{10}$ showing molybdenum oxide polyhedra[197] and $[Ag_{27}@(Si_2W_{18}O_{66})_3]^{31-}$ showing silicon oxide and tungsten oxide polyhedra.[140] C: grayish bone, O: red, Si: pale blue polyhedron, S: yellow, Mo: reddish gray polyhedron, Ag: pale gray, and W: gray polyhedron. Part A reproduced from CCDC 1960490 and 185824. Part B reproduced from CCDC 1050793 and 1949947.

In conclusion, a comprehensive categorization of clusters based on their constituent chemical elements allowed us to understand which method covered which elements and revealed the common points of the structures synthesized by different methods. It is suggested that blending chemical concepts for stabilizing clusters by combining these methods or introducing them into nanoparticles will enable the synthesis of as-yet-unknown clusters not obtained by conventional techniques, affording us many bridgeheads for the next stage of developing cluster fields. Finally, the one-size-fits-all synthetic method constructed using such an approach is a new strategy to promote this cluster chemistry to a more central and larger chemistry field in the future, leading to the creation of next-generation functional materials, such as quantum-sized catalysts.

Author contributions

T. T. composed the entire manuscript.

Conflicts of interest

There are no conflicts of interest to declare.

Acknowledgements

The author acknowledges grants from JST PRESTO Grant Number JPMJPR20AA, JSPS KAKENHI Grant Number JP22H01904, the Advanced Technology Institute, the Yoshinori Ohsumi Fund for Fundamental Research, the JGC-Saneyoshi Scholarship Foundation, the Toshiaki Ogasawara Memorial Foundation, the Iwatani Naoji Foundation, the Inamori Foundation, Mizuho Foundation for the Promotion of Sciences, Iketani Science and Technology Foundation, and the Special Fund of Institute of Industrial Science, University of Tokyo. Drawings of the crystal structures of the clusters were reproduced using VESTA[214] according to the Cambridge Crystallographic Data Centre (CCDC) database.

References

1 M. Naito, T. Yokoyama, K. Hosokawa and K. Nogi, *Nanoparticle Technology Handbook*, Elsevier, 3rd edn, 2018.
2 C. Burda, X. Chen, R. Narayanan and M. A. El-Sayed, Chemistry and properties of nanocrystals of different shapes, *Chem. Rev.*, 2005, **105**, 1025–1102.
3 K. D. Gilroy, A. Ruditskiy, H.-C. Peng, D. Qin and Y. Xia, Bimetallic nanocrystals: syntheses, properties, and applications, *Chem. Rev.*, 2016, **116**, 10414–10472.
4 M. Arndt, O. Nairz, J. Vos-Andreae, C. Keller, G. van der Zouw and A. Zeilinger, Wave–particle duality of C_{60} molecules, *Nature*, 1999, **401**, 680–682.
5 M. Haruta, When gold is not noble: catalysis by nanoparticles, *Chem. Rec.*, 2003, **3**, 75–87.
6 T. Tsukamoto, N. Haruta, T. Kambe, A. Kuzume and K. Yamamoto, Periodicity of molecular clusters based on symmetry-adapted orbital model, *Nat. Commun.*, 2019, **10**, 3727.
7 N. Haruta, T. Tsukamoto, A. Kuzume, T. Kambe and K. Yamamoto, Nanomaterials design for super-degenerate electronic state beyond the limit of geometrical symmetry, *Nat. Commun.*, 2018, **9**, 3758.
8 T. Tsukamoto, T. Kambe, T. Imaoka and K. Yamamoto, Modern cluster design based on experiment and theory, *Nat. Rev. Chem.*, 2021, **5**, 338–347.
9 J. Yano and V. Yachandra, Mn_4Ca cluster in photosynthesis: where and how water is oxidized to dioxygen, *Chem. Rev.*, 2014, **114**, 4175–4205.
10 D. C. Johnson, D. R. Dean, A. D. Smith and M. K. Johnson, Structure, function, and formation of biological iron–sulfur clusters, *Annu. Rev. Biochem.*, 2005, **74**, 247–281.
11 C. V. Stappen, L. Decamps, G. E. Cutsail III, R. Bjornsson, J. T. Henthorn, J. A. Birrell and S. DeBeer, The Spectroscopy of Nitrogenases, *Chem. Rev.*, 2020, **120**, 5005–5081.
12 Z. Gai, A. Matsuno, K. Kato, S. Kato, M. R. I. Khan, T. Shimizu, T. Yoshioka, Y. Kato, H. Kishimura, G. Kanno, Y. Miyabe, T. Terada, Y. Tanaka and M. Yao, Crystal structure of the 3.8-MDa respiratory supermolecule hemocyanin at 3.0 A° resolution, *Structure*, 2015, **23**, 2204–2212.
13 H. Komori and Y. Higuchi, Structural insights into the O_2 reduction mechanism of multicopper oxidase, *J. Biochem.*, 2015, **158**, 293–298.
14 P. J. Dyson and J. S. McIndoe, *Transition metal carbonyl cluster chemistry*, CRC Press, 1st edn, 2000, vol. 2, Advanced chemistry texts.
15 K. Wade, Structural and bonding patterns in cluster chemistry, *Adv. Inorg. Chem. Radiochem.*, 1976, **18**, 1–66.
16 D. M. P. Mingos, Polyhedral skeletal electron pair approach, *Acc. Chem. Res.*, 1984, **17**, 311–319.
17 E. D. Jemmis and E. G. Jayasree, Analogies between boron and carbon, *Acc. Chem. Res.*, 2003, **36**, 816–824.
18 H. W. Kroto, J. R. Heath, S. C. O'Brien, R. F. Curl and R. E. Smalley, C_{60}: Buckminsterfullerene, *Nature*, 1985, **318**, 162–163.
19 S. Liu, Y.-J. Lu, M. M. Kappes and J. A. Ibers, The structure of the C_{60} molecule: X-ray crystal structure determination of a twin at 110K, *Science*, 1991, **254**, 408–410.
20 A. Astefanei, O. Núñez and M. T. Galceran, Characterisation and determination of fullerenes: A critical review, *Anal. Chim. Acta*, 2015, **882**, 1–21.
21 S. Guha and K. Nakamoto, Electronic structures and spectral properties of endohedral fullerenes, *Coord. Chem. Rev.*, 2005, **249**, 1111–1132.

22 A. A. Popov, S. Yang and L. Dunsch, Endohedral fullerenes, *Chem. Rev.*, 2013, **113**, 5989–6113.
23 M. D. Morse, Clusters of transition-metal atoms, *Chem. Rev.*, 1986, **86**, 1049–1109.
24 W. D. Knight, K. Clemenger, W. A. de Heer, W. A. Saunders, M. Y. Chou and M. L. Cohen, Electronic shell structure and abundances of sodium clusters, *Phys. Rev. Lett.*, 1984, **52**, 2141–2143.
25 D. E. Bergeron, A. W. Castleman, T. Morisato and S. N. Khanna, Formation of $Al_{13}I^-$: evidence for the superhalogen character of Al_{13}, *Science*, 2004, **304**, 84–87.
26 L.-F. Cui, X. Huang, L.-M. Wang, J. Li and L.-S. Wang, Endohedral stannaspherenes $M@Sn_{12}^-$: a rich class of stable molecular cage clusters, *Angew. Chem., Int. Ed.*, 2007, **46**, 742–745.
27 H.-J. Zhai, Y.-F. Zhao, W.-L. Li, Q. Chen, H. Bai, H.-S. Hu, Z. A. Piazza, W.-J. Tian, H.-G. Lu, Y.-B. Wu, Y.-W. Mu, G.-F. Wei, Z.-P. Liu, J. Li, S.-D. Li and L.-S. Wang, Observation of an all-boron fullerene, *Nat. Chem.*, 2014, **6**, 727–731.
28 J. Li, X. Li, H.-J. Zhai and L.-S. Wang, Au_{20}: a tetrahedral cluster, *Science*, 2003, **299**, 864–867.
29 K. Koyasu, M. Akutsu, M. Mitsui and A. Nakajima, Selective formation of MSi_{16} (M = Sc, Ti, and V), *J. Am. Chem. Soc.*, 2005, **127**, 4998–4999.
30 M. Mitsui, S. Nagaoka, T. Matsumoto and A. Nakajima, Soft-landing isolation of vanadium–benzene sandwich clusters on a room- temperature substrate using n-alkanethiolate self- assembled monolayer matrixes, *J. Am. Chem. Soc.*, 2006, **110**, 2968–2971.
31 C. A. Schalley, G. Hornung, D. Schröder and H. Schwarz, Mass spectrometric approaches to the reactivity of transient neutrals, *Chem. Soc. Rev.*, 1998, **27**, 91–104.
32 S. Takano, S. Hasegawa, M. Suyama and T. Tsukuda, Hydride doping of chemically modified gold-based superatoms, *Acc. Chem. Res.*, 2018, **51**, 3074–3083.
33 R. Jin, C. Zeng, M. Zhou and Y. Chen, Atomically precise colloidal metal nanoclusters and nanoparticles: fundamentals and opportunities, *Chem. Rev.*, 2016, **116**, 10346–10413.
34 I. Chakraborty and T. Pradeep, Atomically precise clusters of noble metals: emerging link between atoms and nanoparticles, *Chem. Rev.*, 2017, **117**, 8208–8271.
35 Q. Yao, T. Chen, X. Yuan and J. Xie, Toward total synthesis of thiolate- protected metal nanoclusters, *Acc. Chem. Res.*, 2018, **51**, 1338–1348.
36 S. Sharma, K. K. Chakrahari, J.-Y. Saillard and C. W. Liu, Structurally precise dichalcogenolateprotected copper and silver superatomic nanoclusters and their alloys, *Acc. Chem. Res.*, 2018, **51**, 2475–2483.
37 Y. Negishi, W. Kurashige and U. Kamimura, Isolation and structural characterization of an octaneselenolate-protected Au_{25} cluster, *Langmuir*, 2011, **27**, 12289–12292.
38 M. G. Taylor and G. Mpourmpakis, Thermodynamic stability of ligand-protected metal nanoclusters, *Nat. Commun.*, 2017, **8**, 15988.
39 P. D. Jadzinsky, G. Calero, C. J. Ackerson, D. A. Bushnell and R. D. Kornberg, Structure of a thiol monolayer-protected gold nanoparticle at 1.1 Å resolution, *Science*, 2007, **318**, 430–433.
40 H. Qian and R. Jin, Controlling nanoparticles with atomic precision: The case of $Au_{144}(SCH_2CH_2Ph)_{60}$, *Nano Lett.*, 2009, **9**, 4083–4087.
41 H.-C. Weissker, H. Escobar, V. D. Thanthirige, K. Kwak, D. Lee, G. Ramakrishna, R. L. Whetten and X. López-Lozano, Information on quantum states pervades the visible spectrum of the ubiquitous $Au_{144}(SR)_{60}$ gold nanocluster, *Nat. Commun.*, 2014, **5**, 3785.
42 Z. Wang, H.-F. g. Su, Y.-Z. Tan, S. Schein, S.-C. Lin, W. Liu, S.-A. Wang, W.-G. Wang, C.-H. Tung, D. Sun and L.-S. Zheng, Assembly of silver Trigons into a buckyball-like Ag_{180} nanocage, *Proc. Natl. Acad. Sci. U. S. A.*, 2017, **114**, 12132–12137.
43 H. Yang, Y. Wang, X. Chen, X. Zhao, L. Gu, H. Huang, J. Yan, C. Xu, G. Li, J. Wu, A. J. Edwards, B. Dittrich, Z. Tang, D. Wang, L. Lehtovaara, H. Häkkinen and N. Zheng, Plasmonic twinned silver nanoparticles with molecular precision, *Nat. Commun.*, 2016, **7**, 12809.
44 H. Yang, Y. Wang, H. Huang, L. Gell, L. Lehtovaara, S. Malola, H. Häkkinen and N. Zheng, All-thiol-stabilized Ag_{44} and $Au_{12}Ag_{32}$ nanoparticles with single-crystal structures, *Nat. Commun.*, 2013, **4**, 2422.
45 S. Hossain, Y. Niihori, L. V. Nair, B. Kumar, W. Kurashige and Y. Negishi, Alloy clusters: Precise synthesis and mixing effects, *Acc. Chem. Res.*, 2018, **51**, 3114–3124.
46 W. Fei, S. Antonello, T. Dainese, A. Dolmella, M. Lahtinen, K. Rissanen, A. Venzo and F. Maran, Metal doping of $Au_{25}(SR)_{18}^-$ clusters: Insights and hindsights, *J. Am. Chem. Soc.*, 2019, **141**, 16033–16045.
47 S. K. Barik, C.-Y. Chen, T.-H. Chiu, Y.-R. Ni, F. Gam, I. Chantrenne, S. Kahlal, J.-Y. Saillard and C. W. Liu, Surface modifications of eight-electron palladium silver superatomic alloys, *Commun. Chem.*, 2022, **5**, 151.
48 Y. Horita, M. Ishimi and Y. Negishi, Anion-templated silver nanoclusters: precise synthesis and geometric structure, *Sci. Technol. Adv. Mater.*, 2023, **24**, 2203832.
49 C. W. Liu, H.-W. Chang, C.-S. Fang, B. Sarkar and J.-C. Wang, Anion-templated syntheses of octanuclear silverclusters from a silver dithiophosphate chain, *Chem. Commun.*, 2010, **46**, 4571–4573.
50 J.-H. Liao, H.-W. Chang, Y.-J. Li, C.-S. Fang, B. Sarkar, W. E. van Zyl and C. W. Liu, Anion templating from a silver(I) dithiophosphate 1D polymer forming discrete cationic and neutral octa- and decanuclear silver(I) clusters, *Dalton Trans.*, 2014, **43**, 12380–12389.
51 H. J. Schugar, C. Ou, J. A. Thich, J. A. Potenza, R. A. Lalancette and W. Furey Jr., Molecular structure and copper(II)-mercaptide charge-transfer spectra of a novel $Cu_{14}[SC(CH_3)_2CH_2NH_2]_{12}Cl$ cluster, *J. Am. Chem. Soc.*, 1976, **98**, 3047–3048.
52 C. Zhang, T. Matsumoto, M. Samoc, S. Petrie, S. Meng, T. C. Corkery, R. Stranger, J. Zhang, M. G. Humphrey and

K. Tatsumi, Dodecanuclear-ellipse and decanuclear-wheel nickel(II) thiolato clusters with efficient femtosecond nonlinear absorption, *Angew. Chem., Int. Ed.*, 2010, **49**, 4209–4212.

53 J. Chen, L. Liu, L. Weng, Y. Lin, L. Liao, C. Wang, J. Yang and Z. Wu, Synthesis and properties evolution of a family of tiara-like phenylethanethiolated palladium nanoclusters, *Sci. Rep.*, 2015, **5**, 16628.

54 T. Imaoka, Y. Akanuma, N. Haruta, S. Tsuchiya, K. Ishihara, T. Okayasu, W.-J. Chun, M. Takahashi and K. Yamamoto, Platinum clusters with precise numbers of atoms for preparative-scale catalysis, *Nat. Commun.*, 2017, **8**, 688.

55 Y. Yamashina, Y. Kataoka and Y. Ura, Inclusion of an iodine molecule in a tiara-like octanuclear palladium thiolate complex, *Eur. J. Inorg. Chem.*, 2014, **2014**, 4073–4078.

56 Y. Akanuma, T. Imaoka, H. Sato and K. Yamamoto, Silver in the center enhances room-temperature phosphorescence of a platinum sub-nanocluster by 18 times, *Angew. Chem., Int. Ed.*, 2021, **60**, 4551–4554.

57 A. Eichhöfer, P. T. Wood, R. N. Viswanath and R. A. Mole, Synthesis, structure and physical properties of the manganese(II) selenide/selenolate cluster complexes $[Mn_{32}Se_{14}(SePh)_{36}(PnPr_3)_4]$ and $[Na(benzene\text{-}15\text{-}crown\text{-}5)(C_4H_8O)_2]_2[Mn_8Se(SePh)_{16}]$, *Chem. Commun.*, 2008, 1596–1598.

58 G. Christou, K. S. Hagen and R. H. Holm, Synthesis, structure, and properties of $[Co_8S_6(SC_6H_5)_8]^{4-}$ containing an octanuclear Co8S6 rhombic dodecahedron related to that of cobalt pentlandite, *J. Am. Chem. Soc.*, 1982, **104**, 1744–1745.

59 I. G. Dance, A. Choy and M. L. Scudder, Syntheses, properties, and molecular and crystal structures of $(Me_4N)_4[E_4M_{10}(SPh)_{16}]$ (E = sulfur or selenium; M = zinc or cadmium): molecular supertetrahedral fragments of the cubic metal chalcogenide lattice, *J. Am. Chem. Soc.*, 1984, **106**, 6285–6295.

60 T. I. Levchenko, B. E. G. Lucier, J. F. Corrigan and Y. Huang, Crystalline superlattices of nanoscopic CdS molecular clusters: An x-ray crystallography and ^{111}Cd SSNMR spectroscopy study, *Inorg. Chem.*, 2018, **57**, 204–217.

61 K. K. Singh, A. Bhattacharyya, S. Havenridge, M. Ghabin, H. Ausmann, M. A. Siegler, C. M. Aikens and A. Das, A first glance into mixed phosphine–stibine moieties as protecting ligands for gold clusters, *Nanoscale*, 2023, **15**, 6934–6940.

62 R. H. Adnan, J. M. L. Madridejos, A. S. Alotabi, G. F. Metha and G. G. Andersson, A review of state of the art in phosphine ligated gold clusters and application in catalysis, *Adv. Sci.*, 2022, **9**, 2105692.

63 C. A. McCandler, J. C. Dahl and K. A. Persson, Phosphine-stabilized hidden ground states in gold clusters investigated via a $Au_n(PH_3)_m$ database, *ACS Nano*, 2023, **17**, 1012–1021.

64 S. Liu, M. S. Eberhart, J. R. Norton, X. Yin, M. C. Neary and D. W. Paley, Cationic copper hydride clusters arising from oxidation of $(Ph_3P)_6Cu_6H_6$, *J. Am. Chem. Soc.*, 2017, **139**, 7685–7688.

65 T. Nakajima, K. Nakamae, Y. Ura and T. Tanase, Multinuclear copper hydride complexes supported by polyphosphine ligands, *Eur. J. Inorg. Chem.*, 2020, **2020**, 2211–2226.

66 A. J. Touchton, G. Wu and T. W. Hayton, Generation of a Ni_3 phosphinidene cluster from the Ni(0) synthon, $Ni(\eta^3\text{-}CPh_3)_2$, *Organometallics*, 2020, **39**, 1360–1365.

67 S.-S. Zhang, L. Feng, R. D. Senanayake, C. M. Aikens, X.-P. Wang, Q.-Q. Zhao, C.-H. Tung and D. Sun, Diphosphine-protected ultrasmall gold nanoclusters: opened icosahedral Au_{13} and heart-shaped Au_8 clusters, *Chem. Sci.*, 2018, **9**, 1251–1258.

68 J. Chen, Q.-F. Zhang, P. G. Williard and L.-S. Wang, Synthesis and Structure Determination of a New Au_{20} Nanocluster Protected by Tripodal Tetraphosphine Ligands, *Inorg. Chem.*, 2014, **53**, 3932–3934.

69 T. Tanase, R. Otaki, T. Nishida, H. Takenaka, Y. Takemura, B. Kure, T. Nakajima, Y. Kitagawa and T. Tsubomura, Strongly luminous tetranuclear gold(I) complexes supported by tetraphosphine ligands, meso- or rac-Bis[(diphenylphosphinomethyl)phenylphosphino] methane, *Chem. – Eur. J.*, 2014, **20**, 1577–1596.

70 K. Nakamae, Y. Takemura, B. Kure, T. Nakajima, Y. Kitagawa and T. Tanase, Self-alignment of low-valent octanuclear palladium atoms, *Angew. Chem., Int. Ed.*, 2015, **54**, 1016–1021.

71 A. Zavras, A. Mravak, M. Bužančić, J. M. White, V. Bonačić-Koutecký and R. A. J. O'Hair, Structure of the ligated Ag_{60} nanoparticle $[\{Cl@Ag_{12}\}@Ag_{48}(dppm)_{12}]$ (where dppm=bis(diphenylphosphino)methane), *Chin. J. Chem. Phys.*, 2019, **32**, 182–186.

72 M. L. Steigerwald, T. Siegrist and S. M. Stuczynski, Octatelluridohexakis(triethylphosphine)hexacobalt and a connection between Chevrel clusters and the NiAs structure, *Inorg. Chem.*, 1991, **30**, 2256–2257.

73 P. C. Ford and A. Vogler, Photochemical and photophysical properties of tetranuclear and hexanuclear clusters of metals with d^{10} and s^2 electronic configurations, *Acc. Chem. Res.*, 1993, **26**, 220–226.

74 M. R. Lichtenthaler, F. Stahl, D. Kratzert, L. Heidinger, E. Schleicher, J. Hamann, D. Himmel, S. Weber and I. Krossing, Cationic cluster formation versus disproportionation of low-valent indium and gallium complexes of 2,2′-bipyridine, *Nat. Commun.*, 2015, **6**, 8288.

75 M. Müller, A. J. Karttunen and M. R. Buchner, Speciation of Be^{2+} in acidic liquid ammonia and formation of tetra- and octanuclear beryllium amido clusters, *Chem. Sci.*, 2020, **11**, 5415–5422.

76 W. Frank, V. Reiland and G. J. Reiβ, $[Bi_2(O_2CCF_3)_4]\cdot C_6Me_6$ - Arene adduct of a reduced main group element carboxylate with paddle wheel structure, *Angew. Chem., Int. Ed.*, 1998, **37**, 2984–2985.

77 F. H. Fry, B. A. Dougan, N. McCann, C. J. Ziegler and N. E. Brasch, Characterization of novel vanadium(III)/

acetate clusters formed in aqueous solution, *Inorg. Chem.*, 2005, **44**, 5197–5199.

78 J. K. Beattie, J. A. Klepetko, A. F. Masters and P. Turner, The chemistry of cobalt acetate. VIII. New members of the family of oxo-centred trimers, $[Co_3(\mu_3\text{-}O)(\mu\text{-}O_2CCH_3)_{5-p}(\mu\text{-}OR)_pL_5]^{2+}$ (R=H, alkyl, L=ligand, p=0–4). The preparation and characterisation of the trimeric tetrakis(μ-acetato)-(μ-hydroxo)-μ_3-oxo-pentakis(pyridine)-tri-cobalt(III) hexafluorophosphate, $[Co_3(\mu_3\text{-}O)(\mu\text{-}O_2CCH_3)_4(\mu\text{-}OH)(C_5H_5N)_5][PF_6]_2$, and the preparation and crystal structure of the trimeric tris(μ-acetato)-(μ-hydroxo)-(μ-methoxo)-μ_3-oxo-pentakis(pyridine)-tri-cobalt(III) hexafluorophosphate·methanol·water solvate $[Co_3(\mu_3\text{-}O)(\mu\text{-}O_2CCH_3)_3(\mu\text{-}OH)(\mu\text{-}OCH_3)(C_5H_5N)_5][PF_6]_2\cdot CH_3OH\cdot 0.25H_2O$, *Polyhedron*, 2003, **22**, 947–965.

79 L. Spanhel, Colloidal ZnO nanostructures and functional coatings: A survey, *J. Sol-Gel Sci. Technol.*, 2006, **39**, 7–24.

80 D. C. Gary, S. E. Flowers, W. Kaminsky, A. Petrone, X. Li and B. M. Cossairt, Single-crystal and electronic structure of a 1.3 nm indium phosphide nanocluster, *J. Am. Chem. Soc.*, 2016, **138**, 1510–1513.

81 A. Schnepf and H. Schnöckel, Metalloid aluminum and gallium clusters: Element modifications on the molecular scale?, *Angew. Chem., Int. Ed.*, 2002, **41**, 3532–3552.

82 A. Ecker, E. Weckert and H. Schnöckel, Synthesis and structural characterization of an Al_{77} cluster, *Nature*, 1997, **387**, 379–381.

83 M. Brynda, R. Herber, P. B. Hitchcock, M. F. Lappert, I. Nowik, P. P. Power, A. V. Protchenko, A. Růžička and J. Steiner, Higher-nuclearity group 14 metalloid clusters: $[Sn_9\{Sn(NRR')\}_6]$, *Angew. Chem., Int. Ed.*, 2006, **45**, 4333–4337.

84 M. H. Chisholm, J. C. Huffman, C. C. Kirkpatrick, J. Leonelli and K. Folting, Metal alkoxides - models for metal oxides. 1. Preparations and structures of hexadecaalkoxytetratungsten compounds, $W_4(OR)_{16}$, where R = Me and Et, and octaoxotetraisopropoxytetrapyridinotetramolybdenum, $Mo_4(O)_4(\mu\text{-}O)_2(\mu^3\text{-}O)_2(O\text{-}i\text{-}Pr)_2(\mu\text{-}O\text{-}i\text{-}Pr)_2(py)_4$, *J. Am. Chem. Soc.*, 1981, **103**, 6093–6099.

85 C. Elschenbroich, *Organometallics*, Wiley-VCH Verlag GmbH & Co. KGaA, Weinheim, 5th edn, 2016.

86 H. Wadepohl and S. Gebert, (Cyclopentadienyl) metal cluster complexes of the group 9 transition metals, *Coord. Chem. Rev.*, 1995, **143**, 535–609.

87 H. Banh, K. Dilchert, C. Schulz, C. Gemel, R. W. Seidel, R. Gautier, S. Kahlal, J.-Y. Saillard and R. A. Fischer, Atom-precise organometallic zinc clusters, *Angew. Chem., Int. Ed.*, 2016, **55**, 3285–3289.

88 H. Schnöckel, Structures and properties of metalloid Al and Ga clusters open our eyes to the diversity and complexity of fundamental chemical and physical processes during formation and dissolution of metals, *Chem. Rev.*, 2010, **110**, 4125–4153.

89 H. Banh, J. Hornung, T. Kratz, C. Gemel, A. Pöthig, F. Gam, S. Kahlal, J.-Y. Saillard and R. A. Fischer, Embryonic brass: pseudo two electron Cu/Zn clusters, *Chem. Sci.*, 2018, **9**, 8906–8913.

90 J. Weßing, C. Ganesamoorthy, S. Kahlal, R. Marchal, C. Gemel, O. Cador, A. C. H. Da Silva, J. L. F. Da Silva, J.-Y. Saillard and R. A. Fischer, The mackay-type cluster $[Cu_{43}Al_{12}](Cp^*)_{12}$: Open-shell 67-electron superatom with emerging metal-like electronic structure, *Angew. Chem., Int. Ed.*, 2018, **57**, 14630–14634.

91 D. A. Buschmann, H. M. Dietrich, D. Schneider, V. M. Birkelbach, C. Stuhl, K. W. Törnroos, C. Maichle-Mössmer and R. Anwander, Nanoscale organolanthanum clusters: Nuclearity-directing role of cyclopentadienyl and halogenido ligands, *Chem. – Eur. J.*, 2020, **26**, 10834–10840.

92 M. N. Sokolov and P. A. Abramov, Chalcogenide clusters of groups 8–10 noble metals, *Coord. Chem. Rev.*, 2012, **256**, 1972–1991.

93 S. Reisinger, M. Bodensteiner, E. M. Pineda, J. J. W. McDouall, M. Scheer and R. A. Layfield, Addition of pnictogen atoms to chromium(II): synthesis, structure and magnetic properties of a chromium(IV) phosphide and a chromium(III) arsenide, *Chem. Sci.*, 2014, **5**, 2443–2448.

94 S. Heinl, K. Kiefer, G. Balázs, C. Wickleder and M. Scheer, The synthesis of the heterocubane cluster $[\{CpMn\}_4(\mu^3\text{-}P)_4]$ as a tetrahedral shaped starting material for the formation of polymeric coordination compounds, *Chem. Commun.*, 2015, **51**, 13474–13477.

95 Y. Ohki, K. Munakata, Y. Matsuoka, R. Hara, M. Kachi, K. Uchida, M. Tada, R. E. Cramer, W. M. C. Sameera, T. Takayama, Y. Sakai, S. Kuriyama, Y. Nishibayashi and K. Tanifuji, Nitrogen reduction by the Fe sites of synthetic $[Mo_3S_4Fe]$ cubes, *Nature*, 2022, **607**, 86–90.

96 T. Murahashi, R. Inoue, K. Usui and S. Ogoshi, Square tetrapalladium sheet sandwich complexes: cyclononatetraenyl as a versatile face-capping ligand, *J. Am. Chem. Soc.*, 2009, **131**, 9888–9889.

97 M. Teramoto, K. Iwata, H. Yamaura, K. Kurashima, K. Miyazawa, Y. Kurashige, K. Yamamoto and T. Murahashi, Three-dimensional sandwich nanocubes composed of 13-atom palladium core and hexakis-carbocycle shell, *J. Am. Chem. Soc.*, 2018, **140**, 12682–12686.

98 S. Gambarotta, C. Floriani, A. Chiesi-Villa and C. Guastini, A homoleptic arylgold(I) complex: Synthesis and structure of pentanuclear mesitylgold(I), *J. Chem. Soc., Chem. Commun.*, 1983, 1304–1306.

99 E. M. Meyer, S. Gambarotta, C. Floriani, A. Chiesi-Villa and C. Guastini, Polynuclear aryl derivatives of group 11 Metals: Synthesis, solid state-solution structural relationship, and reactivity with phosphines, *Organometallics*, 1989, **8**, 1067–1079.

100 H. Müller, W. Seidel and H. Görls, Zur chemie des dimesityleisens: VI. Die struktur von tetramesityldieisen, *J. Organomet. Chem.*, 1993, **445**, 133–136.

101 X.-L. Pei, A. Pereira, E. S. Smirnova and A. M. Echavarren, Small gold(I) and gold(I)–silver(I) clusters by C–Si auration, *Chem. – Eur. J.*, 2020, **26**, 7309–7313.

102 C. E. Melton, J. W. Dube, P. J. Ragogna, J. C. Fettinger and P. P. Power, Synthesis and characterization of primary

aluminum parent amides and phosphides, *Organometallics*, 2014, **33**, 329–337.

103 Y. Sunada, K. Yamaguchi and K. Suzuki, "Template synthesis" of discrete metal clusters with two- or three-dimensional architectures, *Coord. Chem. Rev.*, 2022, **469**, 214673.

104 T. Yamada, A. Mawatari, M. Tanabe, K. Osakada and T. Tanase, Planar tetranuclear and dumbbell-shaped octanuclear palladium complexes with bridging silylene ligands, *Angew. Chem., Int. Ed.*, 2009, **48**, 568–571.

105 T. Koizumi, K. Tanaka, Y. Tsuchido, M. Tanabe, T. Ide and K. Osakada, Bimolecular fusion of $[Pd_3(\mu\text{-}CN\text{-}C_6H_3Me_2\text{-}2,6)_3(CN\text{-}C_6H_3Me_2\text{-}2,6)_3]$ induced by Ph_2GeH_2: formation of the redox-active Pd_6Ge_2 complex, *Dalton Trans.*, 2019, **48**, 7541–7545.

106 Y. Umehara, R. Usui, Y. Wada and Y. Sunada, Dinuclear and tetranuclear group 10 metal complexes constructed from linear tetrasilane comprising both Si-H and Si-Si moieties, *Commun. Chem.*, 2023, **6**, 93.

107 T. Tsumuraya, Y. Kabe and W. Ando, Synthesis and thermal decomposition, *J. Organomet. Chem.*, 1994, **482**, 131–138.

108 W. P. Neumann and K. Kühlein, Organogermaniumverbindungen, i über diphenylgermanium. octaphenyl-cyclotetragerman, decaphenyl-cyclopentagerman und dodecaphenyl-cyclohexagerman, *Justus Liebigs Ann. Chem.*, 1965, **683**, 1–11.

109 L. Roß and M. Dräger, Phases of Decaphenylcyclopentagermane $(Ph_2Ge)_5$, *Z. Naturforsch., B: J. Chem. Sci.*, 2014, **38**, 665–673.

110 G. Maier, S. Pfriem, U. Schäfer and R. Matusch, Tetra-tert-butyltetrahedrane, *Angew. Chem., Int. Ed. Engl.*, 1978, **17**, 520–521.

111 N. Wiberg, C. M. M. Finger and K. Polborn, Tetrakis(tri-tert-butylsilyl)-tetrahedro-tetrasilane $(t,Bu_3Si)_4Si_4$: The first molecular silicon compound with a Si_4 tetrahedron, *Angew. Chem., Int. Ed. Engl.*, 1993, **32**, 1054–1056.

112 V. G. Albano, L. Grossi, G. Longoni, M. Monari, S. Mulley and A. Sironi, Synthesis and characterization of the paramagnetic $[Ag_{13}Fe_8(CO)_{32}]^{4-}$ tetraanion: A cuboctahedral Ag_{13} cluster stabilized by $Fe(CO)_4$ groups behaving as four-electron donors, *J. Am. Chem. Soc.*, 1992, **114**, 5708–5713.

113 C. Femoni, T. Funaioli, M. C. Iapalucci, S. Ruggieri and S. Zacchini, Rh–Sb nanoclusters: synthesis, structure, and electrochemical studies of the atomically precise $[Rh_{20}Sb_3(CO)_{36}]^{3-}$ and $[Rh_{21}Sb_2(CO)_{38}]^{5-}$ carbonyl compounds, *Inorg. Chem.*, 2020, **59**, 4300–4310.

114 R. H. Sánchez, A. M. Willis, S.-L. Zheng and T. A. Betley, Synthesis of well-defined bicapped octahedral iron clusters $[(^{tren}L)_2Fe_8(PMe_2Ph)_2]_n$ (n=0, −1), *Angew. Chem., Int. Ed.*, 2015, **54**, 12009–12013.

115 R. Wolf and W. Uhl, Main-group-metal clusters stabilized by N-heterocyclic carbenes, *Angew. Chem., Int. Ed.*, 2009, **48**, 6774–6776.

116 T. Kruczyński, F. Henke, M. Neumaier, K. H. Bowen and H. Schnöckel, Many Mg–Mg bonds form the core of the $Mg_{16}Cp^*_8Br_4K$ cluster anion: the key to a reassessment of the Grignard reagent (GR) formation process?, *Chem. Sci.*, 2016, **7**, 1543–1547.

117 M. Schütz, M. Muhr, K. Freitag, C. Gemel, S. Kahlal, J.-Y. Saillard, A. C. H. Da Silva, J. L. F. Da Silva, T. F. Fässler and A. Roland, Fischer, Contrasting Structure and Bonding of a Copper-Rich and a Zinc-Rich Intermetalloid Cu/Zn Cluster, *Inorg. Chem.*, 2020, **59**, 9077–9085.

118 R. D. Adams, M. Chen and X. Yang, Iridium–gold cluster compounds: Syntheses, structures, and an unusual ligand-induced skeletal rearrangement, *Organometallics*, 2012, **31**, 3588–3598.

119 N. de Silva and L. F. Dahl, Synthesis and structural analysis of the first nanosized platinum–gold carbonyl/phosphine cluster, $Pt_{13}[Au_2(PPh_3)_2]_2(CO)_{10}(PPh_3)_4$, containing a Pt-centered $[Ph_3PAu–AuPPh_3]$-capped icosahedral Pt_{12} cage, *Inorg. Chem.*, 2005, **44**(26), 9604–9606.

120 E. G. Mednikov, M. C. Jewell and L. F. Dahl, Nanosized $(\mu_{12}\text{-}Pt)Pd_{164(-x}Pt_x(CO)_{72}(PPh_3)_{20}$ ($x \approx 7$) containing Pt-centered four-shell 165-atom Pd–Pt core with unprecedented intershell bridging carbonyl ligands: Comparative analysis of icosahedral shell-growth patterns with geometrically related $Pd_{145}(CO)_x(PEt_3)_{30}$ ($x \approx 60$) containing capped three-shell Pd_{145} core, *J. Am. Chem. Soc.*, 2007, **129**, 11619–11630.

121 J. Yan, S. Malola, C. Hu, J. Peng, B. Dittrich, B. K. Teo, H. Häkkinen, L. Zheng and N. Zheng, Co-crystallization of atomically precise metal nanoparticles driven by magic atomic and electronic shells, *Nat. Commun.*, 2018, **9**, 3357.

122 J. S. Kanady, E. Y. Tsui, M. W. Day and T. Agapie, A synthetic model of the Mn_3Ca subsite of the oxygen-evolving complex in photosystem II, *Science*, 2011, **333**, 733–736.

123 M. Kato, T. Fukui, H. Sato, Y. Shoji and T. Fukushima, Capturing the trajectory of metal-ion-cluster formation: Stepwise accumulation of Zn(II) ions in a robust coordination space formed by a rigid tridentate carboxylate ligand, *Inorg. Chem.*, 2022, **8**, 3649–3654.

124 N. Araki, K. Kusada, S. Yoshioka, T. Sugiyama, T. Ina and H. Kitagawa, Observation of the formation processes of hexagonal close-packed and face-centered cubic Ru nanoparticles, *Chem. Lett.*, 2019, **48**, 1062–1064.

125 H. J. Lunk and H. Hartl, The fascinating polyoxometalates, *ChemTexts*, 2021, **7**, 26.

126 A. V. Anyushin, A. Kondinski and T. N. Parac-Vogt, Hybrid polyoxometalates as post-functionalization platforms: from fundamentals to emerging applications, *Chem. Soc. Rev.*, 2020, **49**, 382–432.

127 N. I. Gumerova and A. Rompel, Polyoxometalates in solution: speciation under spotlight, *Chem. Soc. Rev.*, 2020, **49**, 7568–7601.

128 A. Müller, S. K. Das, V. P. Fedin, E. Krickemeyer, C. Beugholt, H. Bögge, M. Schmidtmann and B. Hauptfleisch, Rapid and simple isolation of the crystalline molybdenum-blue compounds with discrete and linked nanosized ring-shaped anions: $Na_{15}[MoVI_{126}MoV_{28}$

$O_{462}H_{14}(H_2O)_{70}]_{0.5}[MoVI_{124}MoV_{28}O_{457}H_{14}(H_2O)_{68}]_{0.5}$·ca.400 H_2O and $Na_{22}[MoVI_{118}MoV_{28}O_{442}H_{14}(H_2O)_{58}]$·ca. 250 H_2O, *Z. Anorg. Allg. Chem.*, 1999, **625**, 1187–1192.

129 A. Müller, B. Botar, S. K. Das, H. Bögge, M. Schmidtmann and A. Merca, On the complex hedgehog-shaped cluster species containing 368 Mo atoms: simple preparation method, new spectral details and information about the unique formation, *Polyhedron*, 2004, **23**, 2381–2385.

130 P. C. Burns, K.-A. Kubatko, G. Sigmon, B. J. Fryer, J. E. Gagnon, M. R. Antonio and L. Soderholm, Actinyl peroxide nanospheres, *Angew. Chem., Int. Ed.*, 2005, **44**, 2135–2139.

131 G. E. Sigmon, D. K. Unruh, J. Ling, B. Weaver, M. Ward, L. Pressprich, A. Simonetti and P. C. Burns, Symmetry versus minimal pentagonal adjacencies in uranium-based polyoxometalate fullerene topologies, *Angew. Chem., Int. Ed.*, 2009, **48**, 2737–2740.

132 H. Zhang, A. Li, K. Li, Z. Wang, X. Xu, Y. Wang, M. V. Sheridan, H.-S. Hu, C. Xu, E. V. Alekseev, Z. Zhang, P. Yan, K. Cao, Z. Chai, T. E. Albrecht-Schönzart and S. Wang, Ultrafiltration separation of Am(VI)-polyoxometalate from lanthanides, *Nature*, 2023, **616**, 482–487.

133 A. Blazevic and A. Rompel, The Anderson–Evans polyoxometalate: From inorganic building blocks via hybrid organic–inorganic structures to tomorrows "Bio-POM", *Coord. Chem. Rev.*, 2016, **307**, 42–64.

134 D. D. Dexter and J. V. Silverton, A new structural type for heteropoly anions. The crystal structure of $(NH_4)_2H_6(CeMo_{12}O_{42})$·$12H_2O$, *J. Am. Chem. Soc.*, 1968, **90**, 3589–3590.

135 C. Boskovic, Rare earth polyoxometalates, *Acc. Chem. Res.*, 2017, **50**, 2205–2214.

136 S. V. Krivovichev, Polyoxometalate clusters in minerals: review and complexity analysis, *Acta Crystallogr., Sect. B: Struct. Sci., Cryst. Eng. Mater.*, 2020, **76**, 618–629.

137 Y. Sakai, K. Yoza, C. N. Kato and K. Nomiya, Tetrameric, trititanium(IV)-substituted polyoxotungstates with α-Dawson substructure as soluble metal-oxide analogues: Molecular structure of the giant "Tetrapod" $[(\alpha\text{-}1,2,3\text{-}P_2W_{15}Ti_3O_{62})_4\{\mu^3\text{-}Ti(OH)_3\}_4Cl]^{45-}$, *Chem. – Eur. J.*, 2003, **9**, 4077–4083.

138 S. S. Mal and U. Kortz, The wheel-shaped Cu_{20} tungstophosphate $[Cu_{20}Cl(OH)_{24}(H_2O)_{12}(P_8W_{48}O_{184})]^{25-}$ ion, *Angew. Chem., Int. Ed.*, 2005, **44**, 3777–3780.

139 S.-R. Li, H.-Y. Wang, H.-F. Su, H.-J. Chen, M.-H. Du, L.-S. Long, X.-J. Kong and L.-S. Zheng, A giant 3d-4f polyoxometalate super-tetrahedron with high proton conductivity, *Small Methods*, 2021, **5**, 2000777.

140 K. Yonesato, H. Ito, H. Itakura, D. Yokogawa, T. Kikuchi, N. Mizuno, K. Yamaguchi and K. Suzuki, Controlled assembly synthesis of atomically precise ultrastable silver nanoclusters with polyoxometalates, *J. Am. Chem. Soc.*, 2019, **141**, 19550–19554.

141 W. H. Casey, Large aqueous aluminum hydroxide molecules, *Chem. Rev.*, 2006, **106**, 1–16.

142 O. Sadeghi, L. N. Zakharov and M. Nyman, Aqueous formation and manipulation of the iron-oxo Keggin ion, *Science*, 2015, **347**, 1359–1362.

143 G. N. Newton, S. Yamashita, K. Hasumi, J. Matsuno, N. Yoshida, M. Nihei, T. Shiga, M. Nakano, H. Nojiri, W. Wernsdorfer and H. Oshio, Redox-controlled magnetic $\{Mn_{13}\}$ Keggin systems, *Angew. Chem., Int. Ed.*, 2011, **50**, 5716–5720.

144 C. Liu, J. Hu, F. Zhu, J. Zhan, L. Du, C.-H. Tung and Y. Wang, Functionalization of titanium oxide cluster $Ti_{17}O_{24}(O^iC_3H_7)_{20}$ with catechols: Structures and ligand-exchange reactivities, *Chem. – Eur. J.*, 2019, **25**, 14843–14849.

145 C. Eychenne-Baron, F. Ribot and C. Sanchez, New synthesis of the nanobuilding block $\{(BuSn)_{12}O_{14}(OH)_6\}^{2+}$ and exchange properties of $\{(BuSn)_{12}O_{14}(OH)_6\}(O_3SC_6H_4CH_3)_2$, *J. Organomet. Chem.*, 1998, **567**, 137–142.

146 A. Möller, P. Amann, V. Kataev and N. Schittner, The first T5-supertetrahedron in oxide chemistry: $Na_{26}Mn_{39}O_{55}$, *Z. Anorg. Allg. Chem.*, 2004, **630**, 890–894.

147 A. Müller, D.-C. R. Rohlfing, E. Krickemeyer and H. Bögge, Control of the linkage of inorganic fragments of V–O compounds: From cluster shells as carcerands via cluster aggregates to solid-state structures, *Angew. Chem., Int. Ed. Engl.*, 1993, **32**, 909–912.

148 R. Wang, H. D. Selby, H. Liu, M. D. Carducci, T. Jin, Z. Zheng, J. W. Anthis and R. J. Staples, Halide-templated assembly of polynuclear lanthanide-hydroxo complexes, *Inorg. Chem.*, 2002, **41**, 278–286.

149 A. Müller, E. Krickemeyer, S. Dillinger, H. Bögge and A. Stammler, $[As_4Mo_6V_7O_{39}(SO_4)]^{4-}$: A species with an unusual structure and a model for the different host-guest properties of poly-vanadates and -molybdates, *J. Chem. Soc., Chem. Commun.*, 1994, 2539–2540.

150 G. K. Johnson and E. O. Schlemper, Existence and structure of the molecular ion 18-vanadate(IV), *J. Am. Chem. Soc.*, 1978, **100**, 3645–3646.

151 V. W. Day, W. G. Klemperer and O. M. Yaghi, Synthesis and characterization of a soluble oxide inclusion complex, $[CH_3CN\subset(V_{12}O_{32}{}^{4-})]$, *J. Am. Chem. Soc.*, 1989, **111**, 5959–5961.

152 A. Flemming, A. Hoppe and M. Köckerling, Synthesis and structures of new niobium cluster compounds with pyridinium cations: $(PyrH)_2[Nb_6Cl_{18}]$·EtOH (Pyr: pyridine, Et: ethyl) and the cubic modification of $(PyrH)_2[Nb_6Cl_{18}]$, *J. Solid State Chem.*, 2008, **181**, 2660–2665.

153 H. Yang, J. Zhang, M. Luo, W. Wang, H. Lin, Y. Li, D. Li, P. Feng and T. Wu, The largest supertetrahedral oxychalcogenide nanocluster and its unique assembly, *J. Am. Chem. Soc.*, 2018, **140**, 11189–11192.

154 T. Kaib, M. Kapitein and S. Dehnen, Synthesis and crystal structure of $[Li_8(H_2O)_{29}][Sn_{10}O_4S_{20}]$·$2H_2O$. Z, *Anorg. Allg. Chem.*, 2011, **637**, 1683–1686.

155 M. J. Moses, J. C. Fettinger and B. W. Eichhorn, Interpenetrating As_{20} fullerene and Ni_{12} icosahedra in the onion-skin $[As@Ni_{12}@As_{20}]^{3-}$ ion, *Science*, 2003, **300**, 778–780.

156 L. Jongen, A.-V. Mudring and G. Meyer, The molecular solid $Sc_{24}C_{10}I_{30}$: A truncated, hollow T4 supertetrahedron

of iodine filled with a T3 supertetrahedron of scandium that encapsulates the adamantoid cluster Sc_4C_{10}, *Angew. Chem., Int. Ed.*, 2006, **45**, 1886–1889.

157 A. Müller, K. Schmitz, E. Krickemeyer, M. Penk and H. Bögge, $[Pd_2S_{28}]^{4-}$: A 30-membered cage containing an entrapped cation, *Angew. Chem., Int. Ed. Engl.*, 1986, **25**, 453–454.

158 J. F. You, B. S. Snyder, G. C. Papaefthymiou and R. H. Holm, On the molecular solid-state boundary. A cyclic iron-sulfur cluster of nuclearity eighteen: synthesis, structure, and properties, *J. Am. Chem. Soc.*, 1990, **112**, 1067–1076.

159 S. Scharfe, F. Kraus, S. Stegmaier, A. Schier and T. F. Fässler, Zintl ions, cage compounds, and intermetalloid clusters of group 14 and group 15 elements, *Angew. Chem., Int. Ed.*, 2011, **50**, 3630–3670.

160 Z.-C. Dong and J. D. Corbett, Unusual icosahedral cluster compounds: Open-shell $Na_4A_6Tl_{13}$ (A = K, Rb, Cs) and the metallic Zintl phase $Na_3K_8Tl_n$ (How does chemistry work in solids?), *J. Am. Chem. Soc.*, 1995, **117**, 6447–6455.

161 M. Somer, W. Carrillo-Cabrera, E.-M. Peters, K. Peters, M. Kaupp and H. G. von Schnering, The $[Sn_5]^{2-}$ cluster compound $[K\text{-}(2,2,2\text{-crypt})]_2Sn_5$ – synthesis, crystal structure, raman spectrum, and hierarchical relationship to $CaIn_2$, *Z. Anorg. Allg. Chem.*, 1999, **625**, 37–42.

162 A. Spiekermann, S. D. Hoffmann and T. F. Fässler, The Zintl ion $[Pb_{10}]^{2-}$: A rare example of a homoatomic *closo* cluster, *Angew. Chem., Int. Ed.*, 2006, **45**, 3459–3462.

163 M. Lindsjö, A. Fischer and L. Kloo, Improvements of and Insights into the Isolation of Bismuth Polycations from Benzene Solution – Single-Crystal Structure Determinations of $Bi_8[GaCl_4]_2$ and $Bi_5[GaCl_4]_3$, *Eur. J. Inorg. Chem.*, 2005, **2005**, 670–675.

164 C. Schulz, J. Daniels, T. Bredow and J. Beck, The electrochemical synthesis of polycationic clusters, *Angew. Chem., Int. Ed.*, 2016, **55**, 1173–1177.

165 S. Ahlert, W. Klein, O. Jepsen, O. Gunnarsson, O. K. Andersen and M. Jansen, $Ag_{13}OsO_6$: A silver oxide with interconnected icosahedral Ag_{13}^{4+} clusters and dispersed $[OsO_6]^{4-}$ octahedra, *Angew. Chem., Int. Ed.*, 2003, **42**, 4322–4325.

166 S. Seidel and K. Seppelt, The Cl_4^+ Ion, *Angew. Chem., Int. Ed.*, 2000, **39**, 3923–3925.

167 P. H. Svensson and L. Kloo, Synthesis, structure, and bonding in polyiodide and metal iodide-iodine systems, *Chem. Rev.*, 2003, **103**, 1649–1684.

168 N. V. Tkachenko, X.-W. Zhang, L. Qiao, C.-C. Shu, D. Steglenko, A. MuÇoz-Castro, Z.-M. Sun and A. I. Boldyrev, Spherical aromaticity of all-metal $[Bi@In_8Bi_{12}]^{3-/5-}$ clusters, *Chem. – Eur. J.*, 2020, **26**, 2073–2079.

169 A. R. Eulenstein, Y. J. Franzke, P. Bügel, W. Massa, F. Weigend and S. Dehnen, Stabilizing a metalloid $\{Zn_{12}\}$ unit within a polymetallide environment in $[K_2Zn_{20}Bi_{16}]^{6-}$, *Nat. Commun.*, 2020, **11**, 5122.

170 R. J. Wilson, N. Lichtenberger, B. Weinert and S. Dehnen, Intermetalloid and heterometallic clusters combining p-block (semi)metals with d- or f-block metals, *Chem. Rev.*, 2019, **119**, 8506–8554.

171 B. Kesanli, J. Fettinger, D. R. Gardner and B. Eichhorn, The $[Sn_9Pt_2(PPh_3)]^{2-}$ and $[Sn_9Ni_2(CO)]^{3-}$ complexes: Two markedly different Sn_9M_2L transition metal Zintl ion clusters and their dynamic behaviour, *J. Am. Chem. Soc.*, 2002, **124**, 4779–4786.

172 A. R. Eulenstein, Y. J. Franzke, N. Lichtenberger, R. J. Wilson, H. L. Deubner, F. Kraus, R. Clérac, F. Weigend and S. Dehnen, Substantial π-aromaticity in the anionic heavy-metal cluster $[Th@Bi_{12}]^{4-}$, *Nat. Chem.*, 2021, **13**, 149–155.

173 M. Quintanilla and L. M. Liz-Marzán, Caged clusters shine brighter, *Science*, 2018, **361**, 645.

174 E. Coutiño-Gonzalez, W. Baekelant, J. A. Steele, C. W. Kim, M. B. J. Roeffaers and J. Hofkens, Silver clusters in zeolites: from self- assembly to ground- breaking luminescent properties, *Acc. Chem. Res.*, 2017, **50**, 2353–2361.

175 M. Choi, Z. Wu and E. Iglesia, Mercaptosilane-assisted synthesis of metal clusters within zeolites and catalytic consequences of encapsulation, *J. Am. Chem. Soc.*, 2010, **132**, 9129–9137.

176 N. Wang, Q. Sun, R. Bai, X. Li, G. Guo and J. Yu, In situ confinement of ultrasmall Pd clusters within nanosized silicalite-1 zeolite for highly efficient catalysis of hydrogen generation, *J. Am. Chem. Soc.*, 2016, **138**, 7484–7487.

177 L. Liu, Generation of subnanometric platinum with high stability during transformation of a 2D zeolite into 3D, *Nat. Mater.*, 2017, **16**, 132–138.

178 F. R. Fortea-Pérez, M. Mon, J. Ferrando-Soria, M. Boronat, A. Leyva-Pérez, A. Corma, J. M. Herrera, D. Osadchii, J. Gascon, D. Armentano and E. Pardo, The MOF-driven synthesis of supported palladium clusters with catalytic activity for carbene-mediated chemistry, *Nat. Mater.*, 2017, **16**, 760–766.

179 D. Yang, C. A. Gaggioli, E. Conley, M. Babucci, L. Gagliardi and B. C. Gates, Synthesis and characterization of tetrairidium clusters in the metal organic framework UiO-67: Catalyst for ethylene hydrogenation, *J. Catal.*, 2020, **382**, 165–172.

180 K. Kratzl, T. Kratky, S. Günther, O. Tomanec, R. Zbořil, J. Michalička, J. M. Macak, M. Cokoja and R. A. Fischer, Generation and stabilization of small platinum clusters $Pt_{12\pm x}$ inside a metal–organic framework, *J. Am. Chem. Soc.*, 2019, **141**, 13962–13969.

181 T. Osuga, T. Murase and M. Fujita, Triple-decker Au_3–Ag–Au_3–Ag–Au_3 ion cluster enclosed in a self-assembled cage, *Angew. Chem., Int. Ed.*, 2012, **51**, 12199–12201.

182 T. Kitao, T. Miura, R. Nakayama, Y. Tsutsui, Y. S. Chan, H. Hayashi, H. Yamada, S. Seki, T. Hitosugi and T. Uemura, Synthesis of polyacene by using a metal–organic framework, *Nat. Synth.*, 2023, **2**, 848–854.

183 P. Mal, B. Breiner, K. Rissanen and J. R. Nitschke, White phosphorus is air-stable within a self-assembled tetrahedral capsule, *Science*, 2009, **324**, 1697–1699.

184 S. Matsuno, M. Yamashina, Y. Sei, M. Akita, A. Kuzume, K. Yamamoto and M. Yoshizawa, Exact mass analysis of

sulfur clusters upon encapsulation by a polyaromatic capsular matrix, *Nat. Commun.*, 2017, **8**, 749.
185 B. Maity, S. Abe and T. Ueno, Observation of gold subnanocluster nucleation within a crystalline protein cage, *Nat. Commun.*, 2017, **8**, 14820.
186 R. M. Crooks, M. Zhao, L. Sun, V. Chechik and L. K. Yeung, Dendrimer-encapsulated metal nanoparticles: synthesis, characterization, and applications to catalysis, *Acc. Chem. Res.*, 2001, **34**, 181–190.
187 T. Tsukamoto, T. Kambe, A. Nakao, T. Imaoka and K. Yamamoto, Atom-hybridization for synthesis of polymetallic clusters, *Nat. Commun.*, 2018, **9**, 3873.
188 T. Tsukamoto, T. Imaoka and K. Yamamoto, Unique functions and applications of rigid dendrimers featuring radial aromatic chains, *Acc. Chem. Res.*, 2021, **54**, 4486–4497.
189 T. Tsukamoto, K. Tomozawa, T. Moriai, N. Yoshida, T. Kambe and K. Yamamoto, Highly accurate synthesis of quasi-sub-nanoparticles by dendron-assembled supramolecular templates, *Angew. Chem., Int. Ed.*, 2022, **61**, e202114353.
190 T. Tsukamoto, A. Kuzume, M. Nagasaka, T. Kambe and K. Yamamoto, Quantum materials exploration by sequential screening technique of heteroatomicity, *J. Am. Chem. Soc.*, 2020, **142**, 19078–19084.
191 T. Moriai, T. Tsukamoto, M. Tanabe, T. Kambe and K. Yamamoto, Selective hydroperoxygenation of olefin realized by coinage multimetallic 1-nanometer catalyst, *Angew. Chem., Int. Ed.*, 2020, **59**, 23051–23055.
192 A. Murugadoss, N. Kai and H. Sakurai, Synthesis of bimetallic gold–silver alloy nanoclusters by simple mortar grinding, *Nanoscale*, 2012, **4**, 1280–1282.
193 P. Billik and B. Horváth, Mechanochemical synthesis of the $[Al_{13}O_4(OH)_{24}(H_2O)_{12}]^{7+}$ Keggin ion, *Inorg. Chem. Commun.*, 2008, **11**, 1125–1127.
194 J.-C. Gabriel, K. Boubekeur and P. Batail, Molecular hexanuclear clusters in the system rhenium-sulfur-chlorine: solid state synthesis, solution chemistry, and redox properties, *Inorg. Chem.*, 1993, **32**, 2894–2900.
195 E. G. Tulsky and J. R. Long, Dimensional reduction: a practical formalism for manipulating solid structures, *Chem. Mater.*, 2001, **13**, 1149–1166.
196 Y. Sugimoto, A. Yurtsever, N. Hirayama, M. Abe and S. Morita, Mechanical gate control for atom-by-atom cluster assembly with scanning probe microscopy, *Nat. Commun.*, 2014, **5**, 4360.
197 X.-Y. Li, Y.-Z. Tan, K. Yu, X.-P. Wang, Y.-Q. Zhao, D. Sun and L.-S. Zheng, Atom-Precise polyoxometalate–Ag_2S core–shell nanoparticles, *Chem. – Asian J.*, 2015, **10**, 1295–1298.
198 Z. Wang, H.-F. Su, M. Kurmoo, C.-H. Tung, D. Sun and L.-S. Zheng, Trapping an octahedral Ag_6 kernel in a sevenfold symmetric Ag_{56} nanowheel, *Nat. Commun.*, 2018, **9**, 2094.
199 H. Muramatsu, T. Kambe, T. Tsukamoto, T. Imaoka and K. Yamamoto, Controlled synthesis of Au_{25} superatom using a dendrimer template, *Molecules*, 2022, **27**, 3398.
200 H. J. Hrostowski and R. J. Myers, The microwave spectra, structure, and dipole moment of stable pentaborane, *J. Chem. Phys.*, 1954, **22**, 262–265.
201 J.-T. Zhao and J. D. Corbett, Square pyramidal clusters in La_3In_5 and Y_3In_5. La_3In_5 as a metallic Zintl phase, *Inorg. Chem.*, 1995, **34**, 378–383.
202 V. M. Retivov, E. Y. Matveev, M. V. Lisovskiy, G. A. Razgonyaeva, L. I. Ochertyanova, K. Y. Zhizhin and N. T. Kuznetsov, Nucleophilic substitution in closo-decaborate $[B_{10}H_{10}]^{2-}$ in the presence of carbocations, *Russ. Chem. Bull.*, 2010, **59**, 550–555.
203 I. J. Mavunkal, B. C. Noll, R. Meijboom, A. Muller and T. P. Fehlner, Novel Approach to Multimetal Metallaborane Clusters. Synthesis of Hypoelectronic nido-$Cp^*_3IrRu_2B_5H_9$ from the Reaction of arachno-$Cp^*IrB_3H_9$ with nido-$(Cp^*RuH)_2B_3H_7$, *Organometallics*, 2006, **25**, 2906–2907.
204 R. Ludwig, Water: from clusters to the bulk, *Angew. Chem., Int. Ed.*, 2001, **40**, 1808–1827.
205 A. Hassanpouryouzband, E. Joonaki, M. Vasheghani Farahani, S. Takeya, C. Ruppel, J. Yang, N. J. English, J. M. Schicks, K. Edlmann, H. Mehrabian, Z. M. Aman and B. Tohidi, Gas hydrates in sustainable chemistry, *Chem. Soc. Rev.*, 2020, **49**, 5225–5309.
206 A. Falenty, T. C. Hansen and W. F. Kuhs, Formation and properties of ice XVI obtained by emptying a type sII clathrate hydrate, *Nature*, 2014, **516**, 231–233.
207 K. Momma, T. Ikeda, K. Nishikubo, N. Takahashi, C. Honma, M. Takada, Y. Furukawa, T. Nagase and Y. Kudoh, New silica clathrate minerals that are isostructural with natural gas hydrates, *Nat. Commun.*, 2011, **2**, 196.
208 A. Y. Likhacheva, S. V. Goryainov, Y. V. Seryotkin, K. D. Litasov and K. Momma, Raman spectroscopy of chibaite, natural MTN silica clathrate, at high pressure up to 8 GPa, *Microporous Mesoporous Mater.*, 2016, **224**, 100–106.
209 A. Hirata, L. J. Kang, T. Fujita, B. Klumov, K. Matsue, M. Kotani, A. R. Yavari and M. W. Chen, Geometric frustration of icosahedron in metallic glasses, *Science*, 2013, **341**, 376–379.
210 V. Y. Shevchenko, V. A. Blatov and G. D. Ilyushin, Cluster self-organization of intermetallic systems: New three-layer cluster precursor K136 = $0@Zn_{12}@32(Mg_{20}Zn_{12})@92(Zr_{12}Zn_{80})$ and a new two-layer cluster precursor K30 = $0@Zn_6@Zn_{24}$ in the crystal structure of $Zr_6Mg_{20}Zn_{128}$-cP,154, *Glass Phys. Chem.*, 2020, **46**, 455–461.
211 D. Shechtman, I. Blech, D. Gratias and J. W. Cahn, Metallic phase with long-range orientational order and no translational symmetry, *Phys. Rev. Lett.*, 1984, **53**, 1951–1953.
212 D. Levine and P. J. Steinhardt, Quasicrystals: a new class of ordered structures, *Phys. Rev. Lett.*, 1984, **53**, 2477–2480.
213 H. Takakura, C. P. Gómez, A. Yamamoto, M. De Boissieu and A. P. Tsai, Atomic structure of the binary icosahedral Yb–Cd quasicrystal, *Nat. Mater.*, 2007, **6**, 58–63.
214 K. Momma and F. Izumi, VESTA 3 for three-dimensional visualization of crystal, volumetric and morphology data, *J. Appl. Crystallogr.*, 2011, **44**, 1272–1276.

